Korean J. Chem. Eng., 38(1), 215-225 (2021)
DOI: 10.1007/s11814-020-0681-4

pISSN: 0256-1115
eISSN: 1975-7220

Optimal synthesis of carboxymethylcellulose-based composite superabsorbents

Byungsu Kim[*], **Tak-Hyun Kim**[**], **and Byunghwan Lee**[*,†]

[*]Department of Chemical Engineering, Keimyung University, 1095 Dalgubeoldaero, Dalseo-gu, Daegu 42601, Korea
[**]Advanced Radiation Technology Institute, Korea Atomic Energy Research Institute,
29 Geumgu-gil, Jeongup-si, Jeonbuk 56212, Korea

(*Received 30 July 2020 • Revised 16 September 2020 • Accepted 18 September 2020*)

Abstract–As a liquid fertilizer slow-release material, carboxymethylcellulose-based superabsorbents having biodegradable properties have recently attracted attention. To improve the gel properties of this superabsorbent, which has relatively low mechanical strength, additive materials such as graphite oxide (GO), reduced graphene oxide (rGO), activated carbon, and bentonite were used in this work. While preparing composite superabsorbents using electron beam (EB) radiation, effects of the type and composition of additives, absorbed dose of EB, and type of radiation on the properties of the prepared materials were investigated. In addition, it was attempted to find the optimum synthesis conditions for the preparation of composite superabsorbents. Gel strength and gel fraction were measured to determine the intermolecular binding force of the prepared composite superabsorbents. Swelling tests were carried out in distilled water, urea aqueous solution and NaCl aqueous solution, respectively, to determine the equilibrium swelling ratio and swelling rate in various environments. To examine the applicability of the prepared superabsorents in the field, elution tests were performed using urea as a simulated nitrogen fertilizer. Plant growth experiments were also carried out with spinach and crown daisy to confirm the applicability of the prepared superabsorbents for agricultural purpose. Superabsorbents with GO and rGO showed high gel fraction and high mechanical strength due to the high intermolecular binding force between polymer gel and carbon additive material. In the composite superabsorbents with GO and rGO, gel strength and gel fraction increased with the increase of the amount of inorganic additives, but the equilibrium swelling ratio decreased. Superabsorbents prepared by irradiation of EB at 10 kGy exhibited the highest equilibrium swelling ratio, and the equilibrium swelling ratio decreased as the absorbed dose increased. Furthermore, composite superabsorbents prepared by EB irradiation showed higher gel strength than those prepared by γ-ray irradiation. Plant growth was better in the experimental group containing the superabsorbent and the liquid fertilizer, indicating that the prepared composite superabsorbent could function as a slow-release liquid fertilizer.

Keywords: Carboxymethylcellulose, Graphene, Superabsorbent, Electron Beam, Inorganic Additives

INTRODUCTION

The livestock industry grows due to the increase of meat consumption and the amount of livestock manure that causes environmental pollution is increasing. Livestock manure has been treated by landfilling, marine dumping, and discharge after water treatment. However, these methods have caused many problems, such as soil and sea pollution, eutrophication of rivers, and odor generation [1]. Therefore, recycling processes for livestock manure have attracted much attention. There are two kinds of methods, composting and liquefaction, for the use of livestock manure as an agricultural purpose. More researches have been being actively made on liquefaction than composting due to the superior economic and agricultural advantages [2]. However, the ratio of liquefaction remains at a very low level in the total throughput of livestock manure. The reasons are as follows. i) The odor of the liquid fertilizer made from livestock manure is very severe. ii) Transportation is inconvenient due to the liquid form. iii) A reservoir must be installed to store the liquid, and facilities for storage should be periodically inspected and repaired. iv) About 70% of liquid fertilizer sprayed on land penetrates into groundwater causing groundwater pollution and deteriorating its function as a fertilizer [2]. Therefore, to overcome these drawbacks, it is necessary to use a material capable of slowly releasing the livestock manure.

Recently, superabsorbents have attracted attention as a material capable of absorbing and releasing liquid fertilizer. A superabsorbent is a polymer material that is physically and chemically crosslinked in three dimensions so that its structure and shape are not collapsed as it swells by absorbing water [3]. Superabsorbent absorbs water by the attraction between the hydrophilic functional group and the water molecule, polar bonding between the polymer substance having the anion or cation characteristic and the water molecule, and osmosis due to the difference in concentration between the inside and the outside of the material. Superabsorbents can absorb water up to 1,000 times their own weight. These materials are applied to various fields such as wound dressing, diaper, napkin, contact lens, drug delivery system and soil moisture retention in dry areas [3].

To prepare a superabsorbent, a solution polymerization method has been widely used [4]. However, in solution polymerization, the

---

[†]To whom correspondence should be addressed.
E-mail: leeb@kmu.ac.kr

gelation reaction takes a long time and toxic ingredients can remain in the prepared superabsorbent. Recently, studies on the preparation of superabsorbents by irradiation have been actively carried out to reduce the gelation time and to eliminate toxicity and residuals of pollutants [5]. Electron beam (EB) and γ-ray are mainly used because of the low power consumption. Beta decay of ^{60}Co is generally used to generate γ-rays, and γ-rays can penetrate deeply into the material, allowing mass production of the material. However, γ-ray has disadvantages that the ionizing force is weaker than that of EB and the irradiation time is long [6]. EB is obtained by heating the electron gun and passing the electrons through the acceleration tube and the electromagnet. EB irradiation can control the kinetic energy of the electron by controlling the acceleration of electrons, so that chain cutting and cross-linking of the polymer can be controlled. The irradiation time of EB is short due to the high energy, and EB has strong ionization efficiency. However, it is difficult to apply it to mass production and thick material because the transmittance to the material is about mm unit.

A variety of polymeric materials, including acrylamide or acrylic acid, have been used for superabsorbent production [3,7]. In recent years, many studies have been conducted on the preparation of superabsorbents using biodegradable and nontoxic polymers with less environmental burden. Representative biodegradable polymers include starch, chitosan, and cellulose. Among these materials, cellulose is easy to obtain and not expensive. However, since the molecular structure of cellulose is not suitable for superabsorbent production, sodium carboxymethylcellulose (CMCNa) in which the -OH functional group is substituted with sodium carboxymethyl group is widely used for producing superabsorbents. The superabsorbent made of CMCNa differs in strength and water absorption depending on the degree of substitution (DS) and molecular weight. The higher DS of sodium carboxymethyl group and the lower molecular weight result in higher water absorption but lower mechanical strength. On the contrary, the lower DS and the higher molecular weight result in lower water absorption but higher mechanical strength [8,9].

Additives such as clay and carbon compounds have been used to impart various properties to superabsorbent or to control the swelling ratio and strength. Additives of superabsorbent for liquid fertilizer should be able to improve the strength of the superabsorbent without contaminating soil. Carbon compounds such as activated carbon (AC) or graphene are expected to play this role [10]. Graphene has various properties such as high mechanical strength, flexibility, elasticity, thermal conductivity and electrical conductivity [11]. Due to such excellent physical properties, studies using graphene materials as additives to polyacrylic-based superabsorbents have recently been conducted [12-14]. In this work, graphite oxide was prepared by chemical exfoliation, and then graphene was prepared by thermal expansion and used as additive materials to superabsorbent.

As a precedent research, superabsorbents based on CMCNa were prepared by solution polymerization and EB irradiation, respectively. Gel fraction, swelling ratio and gel strength of the prepared superabsorbents were measured and compared between the two methods. The advantages of EB irradiation were confirmed and the method of preparing superabsorbent using EB was established [15]. Composite superabsorbents, which were obtained by adding graphite oxide (GO), reduced graphene oxide (rGO) and AC to CMCNa, were prepared by EB irradiation, and mechanical strength and swelling ratio were measured. It was confirmed that the mechanical strength of the composite superabsorbent was increased by the addition of GO and rGO [15]. The superabsorbent was also fabricated by varying the composition of the polymer material, and the optimum composition of the polymer was confirmed [16].

In this work, superabsorbents were prepared by using EB while varying the composition of inorganic additive materials to determine the effects of the inorganic additives on the properties of the prepared composite superabsorbents. Gel fraction and mechanical strength were measured to investigate the intermolecular binding force of the composite superabsorbent. Swelling tests were carried out in distilled water, urea aqueous solution and NaCl aqueous solution to determine the maximum absorption and swelling rate in various environments. Urea elution tests were performed to investigate the applicability as a slow-release liquid fertilizer. After establishing the optimal composition of the polymer and inorganic materials of the composite superabsorbent, comparative experiments were conducted to choose the more suitable radiation method between EB and γ-ray. Finally, to confirm the applicability of superabsorbents for agricultural purpose, plant growth experiments were carried out with spinach and crown daisy.

EXPERIMENTAL

1. Materials

Graphite (powder, <20 μm, synthetic, Aldrich, USA), potassium permanganate ($KMnO_4$, ACS reagent, ≥99.0%, Aldrich, USA), sulfuric acid (ACS reagent, 95.0-98.0%, Aldrich, Germany), phosphoric acid (ACS reagent, ≥85 wt% in H_2O, Aldrich, USA), hydrogen peroxide solution (30% in water, Aldrich, USA), ethanol (95%, Samchun, Korea), hydrochloric acid (ACS reagent, 37%, Aldrich, Germany) and diethyl ether ($(C_2H_5)_2O$, 99.5%, Samchun, Korea) were used to make graphite oxide (GO) and reduced graphene oxide (rGO). Sodium carboxymethylcellulose (CMCNa, 99%, ~250,000, 0.7 DS, Aldrich, USA), N,N′-methylenebisacrylamide (NMBA, 99%, Aldrich, USA), activated carbon (AC, ~100 mesh particle size, Aldrich, Netherlands) and bentonite (BT, Aldrich, USA) were used for the preparation of the inorganic composite superabsorbents. For the preparation of all solutions, distilled water was used. Urea (ACS reagent, 99.0-100.5%, Aldrich, Germany) and sodium chloride (NaCl, ACS reagent, ≥99.0%, Aldrich, USA) were used for swelling experiments.

2. Syntheses

GO and rGO used as additives were prepared by the improved Hummers method and the thermal expansion reduction method according to the literature [11,17,18].

Composite superabsorbents were prepared by varying the composition of the inorganic substance as an additive. GO, rGO, AC and BT were used as inorganic additives. First, CMCNa (2.0 g) was dissolved in distilled water (40. mL). An inorganic additive (I) with a mass ratio x relative to CMCNa (x=0.02, 0.05, 0.1, and 0.2) was added to this aqueous solution, stirred to homogeneously mix, and NMBA as a cross-linking agent was added thereto and stirred for 12 hours. The cross-linking agent was added in an amount

Table 1. Compositions of the composite superabsorbents prepared

Sample	CMCNa	Distilled water	Inorganic additive (I)[a]	Cross-linker
C	2.0 g	40. mL	-	0.0420 g
C-$I_{0.02}$			0.04 g	0.0420 g
C-$I_{0.05}$			0.10 g	0.0421 g
C-$I_{0.1}$			0.20 g	0.0422 g
C-$I_{0.2}$			0.40 g	0.0424 g
C-N[b]	2.0 g	40. mL	-	0.0420 g
C-$I_{0.02}$-N			0.04 g	
C-e[c]	20. g	400. mL	-	0.42 g
C-$I_{0.02}$-e			0.40 g	
C-γ			-	
C-$I_{0.02}$-γ			0.40 g	

[a] Inorganic additives (I) used in this work include graphite oxide (GO), reduced graphene oxide (rGO), activated carbon (AC), and bentonite (BT).

[b] N is the irradiation dose of the electron beam used in the preparation, and it includes 10, 20, 30, and 40 kGy.

[c] Electron beam (10 kGy) and γ-ray (10 kGy) were used for the preparation of the samples.

corresponding to 0.1% of the total mass of distilled water, CMCNa, and inorganic additives (Table 1) [19]. The solution was spread on a petri dish with a thickness of 2 mm or less, covered with a plastic wrap, and irradiated with an electron beam (EB) of 30 kGy and 0.7 MeV (ELV-0.5, Russia). The prepared gel was cut into a size of about 1 cm in diameter, piled up into 3 to 4 layers to make it thick, and dried in an oven at 70 °C for 24 hours to obtain an inorganic composite superabsorbent **C-I_x**. A pure polymeric superabsorbent (***C***) to which no inorganic additive was added was also prepared by the same procedure.

Composite superabsorbents were prepared by the same procedure while varying the absorbed dose of EB from 10 kGy to 20 kGy, 30 kGy and 40 kGy (Table 1). The amount of inorganic additive was fixed to the ratio of 0.02 relative to the mass of CMCNa. To easily identify the sample, the absorbed dose of EB irradiation was indicated together with the sample name. For example, the superabsorbent prepared by using GO as an additive and irradiating with EB of 20 kGy was represented by **C-$GO_{0.02}$-20**.

To investigate the effect of the type of radiation on the properties of the composite superabsorbents produced, samples were also prepared by using γ-ray (MDS Nordion, Canada). The same procedure as described above was used with CMCNa (20. g) and distilled water (400. mL). Inorganic additives were added by the ratio of 0.02 to the mass of CMCNa (Table 1). Since γ-ray has a high transmittance, all samples were used as they were in a beaker without an additional pretreatment process. EB and γ-ray were irradiated for 10 minutes and 3 hours with the same absorbed dose of 10 kGy, respectively.

3. Characterization

Structural properties of GO and rGO were determined using Raman spectroscopy (Almega X, Thermo, USA). X-ray diffraction analysis (Pro-MPD, PANalytical, UK) was used to determine the interlayer spacing using CuKα radiation (λ=1.5406 Å). Bragg's equation was used for interlayer spacing calculation. In addition, the surface of GO and rGO prepared was confirmed by scanning electron microscope (SEM, S-4800, Hitachi, Japan). Samples prepared were analyzed by Fourier transform infrared spectroscopy (FTIR, JASCO, FT/IR-620V, Japan) to confirm the binding between CMCNa and inorganic material. FTIR measurements were performed in transmission mode with the samples dispersed in potassium bromide.

4. Gel Properties

4-1. Gel Strength

Gel strength was measured to determine the mechanical strength of the superabsorbent that absorbed the maximum amount of water. Approximately 0.03 g of dry superabsorbent was immersed in distilled water for 24 hours. The superabsorbent having reached the maximum absorption amount was taken out and put in a plastic cell. This cell was placed in a texture analyzer (TEXTplus, MHK Co., Korea) to measure the gel strength under pressure. Gel strength was measured at a pre-test speed of 5 mm/sec, a test speed of 1 mm/sec, a post-test speed of 5 mm/sec, and a trigger force of 5 g.

4-2. Gel Fraction

Gel fraction was measured to determine the intermolecular binding force of the prepared superabsorbent. Approximately 0.02 g of dry superabsorbent was immersed in distilled water for 24 hours. The material was taken out, dried at room temperature for 24 hours, and mass was measured. Gel fraction (G.F.) was determined using the following equation.

$$\mathrm{G.F.}=W_s/W_d\times 100 \tag{1}$$

where W_s represents the mass of the superabsorbent that absorbed distilled water for 24 hours, reached equilibrium, and dried at room temperature, and W_d is the initial mass of the superabsorbent dried before immersion in distilled water.

4-3. Swelling

To determine the maximum absorption and swelling rate of superabsorbent, swelling experiments were carried out using distilled water, urea aqueous solution and NaCl aqueous solution using tea bag method. As a simulated nitrogen liquid fertilizer, urea aqueous solution (50 g/L) was used, and NaCl aqueous solution (9 g/L) was used as physiological saline water [4]. Approximately 0.03 g of dried superabsorbent was placed in a tea bag and carried in an aqueous solution (150 mL). The tea bag was taken out at regular time intervals and the solution on the surface of the tea bag was wiped off with filter paper and the mass was measured. The mass measurement was performed until the weight of the superabsorbent showed no change with time. Swelling ratio was obtained from the following equation.

$$\text{Swelling ratio}=(W_t-W_d)/W_d \tag{2}$$

where W_t represents the mass of swollen superabsorbent at time t.

4-4. Urea Elution

Urea elution characteristics of superabsorbent in aqueous solution were examined as a simulated nitrogen-release from the superabsorbents [19]. Urea aqueous solution 2 mL (10 g/L) was absorbed into 0.03 g of dried superabsorbent. This superabsorbent was dried in a vacuum oven at 70 °C for 24 hours. The dried superabsorbent was immersed in 100 mL of distilled water, and 0.2 mL of the aqueous solution was collected at regular time intervals to measure the urea concentration in the solution. Urea concentration was measured by HPLC (P680 HPLC Pump, UVD170U, DIONEX, USA). For the measurement, YMC-Pack Polymer C18 column (YMC, 6×250 mm, C18, 6 μm) was used and 5 μL of each sample was injected. Mobile phase was distilled water, flow rate was 0.5 mL/min, analysis time was 15 minutes, and the temperature was 30 °C [20].

4-5. Plant Growth

Plant growth experiments were carried out in the laboratory to confirm the field applicability of the prepared superabsorbents. Crown daisy and spinach were chosen for the cultivation experiments because they can grow in a short period of time with no effect of the amount of water on the growth. The livestock liquid fertilizer was provided by a livestock resource recycling center in Y city, Korea. Soils that were burnt at 600 °C for 3 days were used so that the organic matter in the soil did not affect plant growth (soil A). Livestock liquid fertilizer (2 kg) was poured into soil (1 kg) from which organic matter was removed, and the soil was maintained for 10 days while mixing well to obtain soil B. For experiments, soil A (80 g) was mixed with 0.2 g of superabsorbents ***C***, ***C-GO$_{0.2}$***, and ***C-rGO$_{0.2}$***, respectively. For comparison, soil without any superabsorbent was also used in the experiment. Soil B was also used for the experiment in the same manner. A total of eight kinds of soil were used for plant growth experiments. Fluorescent light was used as a light source and 20 mL of distilled water was supplied every day. Plant growth was measured every week for four weeks.

RESULTS AND DISCUSSION

1. Characterization

Raman spectroscopy was used to determine the structural property of the prepared graphite oxide (GO) and reduced graphene oxide (rGO), and the results are shown in Fig. 1. D-band at 1,367.5 cm^{-1}, G-band at 1,512.2 cm^{-1} and 2D-band at 2,748.2 cm^{-1} were observed, indicating that GO and rGO were successfully prepared [15,21]. X-ray diffraction analysis was used to determine the interlayer spacing of the prepared GO and rGO, and the results are shown in Fig. 2. GO showed a strong peak at 9.7°, confirming that the interlayer spacing was 0.92 nm (Fig. 2(a)). The rGO showed a broad graphitic peak at 25.8° (Fig. 2(b)). SEM images of the prepared GO and rGO are shown in Fig. 3. As shown, the interlayer spacing increased and rGO was formed after the reduction GO. All these results indicated that GO and rGO were successfully fabricated [15,18,22].

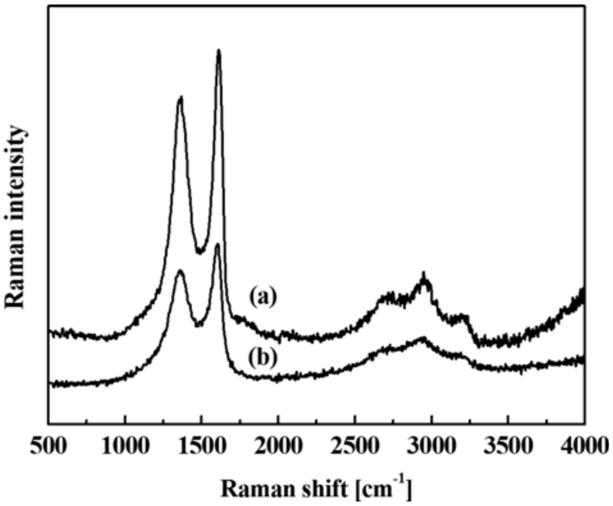

Fig. 1. Raman spectra of the prepared (a) GO and (b) rGO.

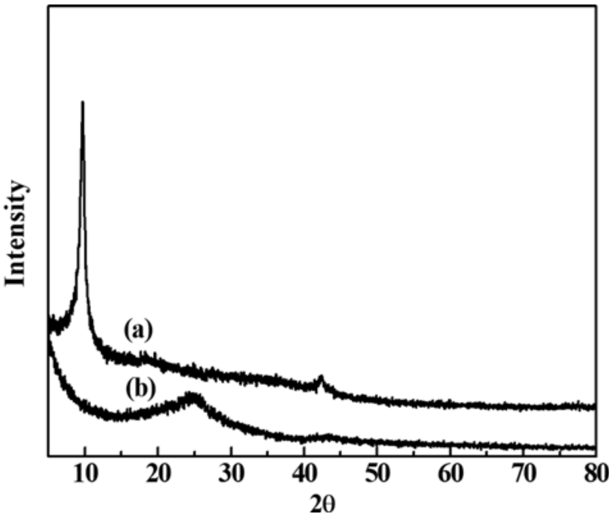

Fig. 2. XRD patterns of (a) GO and (b) rGO.

FTIR analyses were carried out to determine the molecular binding of the prepared composite superabsorbents with different composition of inorganic additives. FTIR analyses were performed on all samples prepared by using GO, rGO, AC and BT as additive materials, and the results of GO-added materials are shown in Fig. 4. The results of analyses of samples using rGO, AC, and BT as additives are shown in the Supporting Information (Fig. S1-Fig. S4). CMC monomer (CMCNa) showed COO$^-$ band at 1,596 cm^{-1}, -CH$_2$ scissoring and COO$^-$ bending band at 1,419 cm^{-1}, -OH bending vibration band at 1,325 cm^{-1} and stretching vibration band of

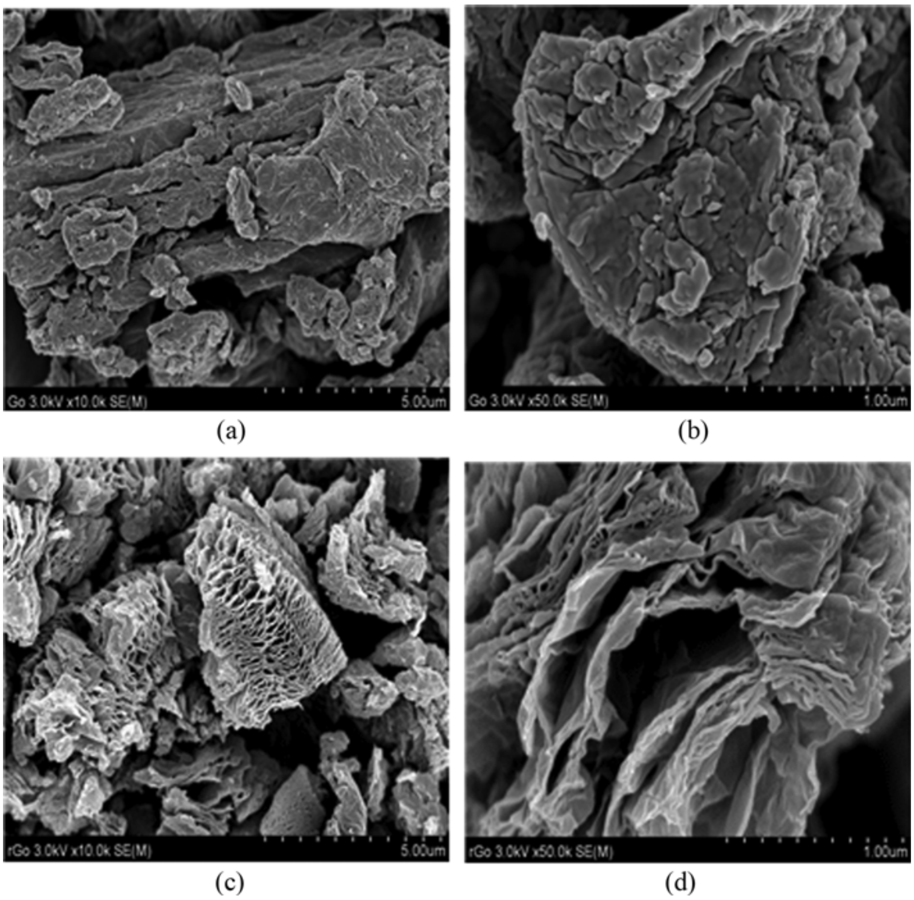

(a) (b)

(c) (d)

Fig. 3. SEM images of GO ((a) and (b)) and rGO ((c) and (d)).

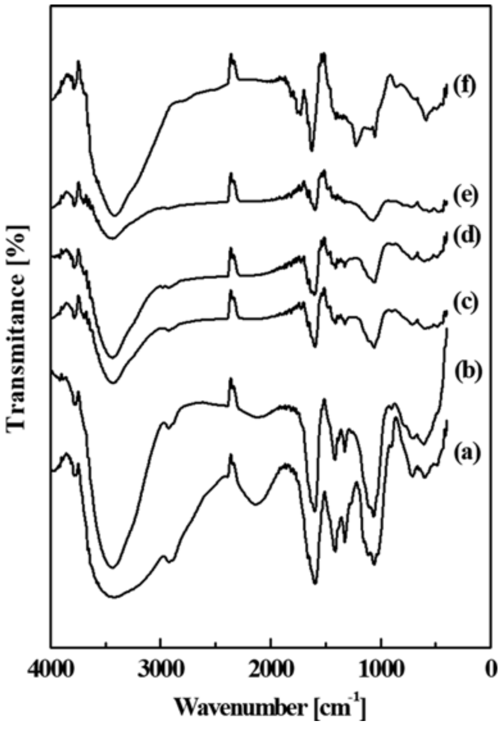

Fig. 4. FTIR spectra of (a) CMCNa, (b) $C\text{-}GO_{0.02}$, (c) $C\text{-}GO_{0.05}$, (d) $C\text{-}GO_{0.1}$, (e) $C\text{-}GO_{0.2}$, and (f) GO.

=CH-O-CH= at 1,057 cm^{-1} (Fig. 4(a)) [15,23]. GO-added composite superabsorbents showed peaks similar to those of CMCNa (Fig. 4). The FTIR analysis result of GO was also shown for comparison (Fig. 4(f)). GO showed a C=O peak at 1,727 cm^{-1}, a C=C peak at 1,628 cm^{-1}, a -C-O-C- peak at 1,225 cm^{-1} and a C-O peak at 1,053 cm^{-1} [19]. As the content of GO contained in the superabsorbents increased, the -CH_2 and COO^- peak at 1,419 cm^{-1} and -OH peak at 1,325 cm^{-1} which were observed in CMCNa decreased. Those peaks disappeared in the spectrum of **$C\text{-}GO_{0.2}$** indicating that CMC polymer and GO formed a complex material (Fig. 4(e)). From these results, it was confirmed that the inorganic materials added were well mixed with the CMC polymer to form a composite superabsorbents.

2. Effect of the Composition of Inorganic Additives on Gel Properties

2-1. Gel Strength

Gel strength measurement experiments were carried out using a texture analyzer to determine the strength of the prepared inorganic composite superabsorbents in the swollen state [24]. The measured values are shown in Fig. 5. The pure polymer, ***C***, withstood a force of 28.1 g. **$C\text{-}GO_{0.02}$** and **$C\text{-}rGO_{0.02}$** resisted 92.7 g and 82.2 g, respectively, while **$C\text{-}GO_{0.2}$** and **$C\text{-}rGO_{0.2}$** withstood a force of 114.1 g and 104.5 g, respectively. From these results, it was found that the gel strength increased as the amount of GO and rGO increased. However, **$C\text{-}AC_{0.02}$** and **$C\text{-}BT_{0.02}$** resisted 23.9 g and 22.3 g,

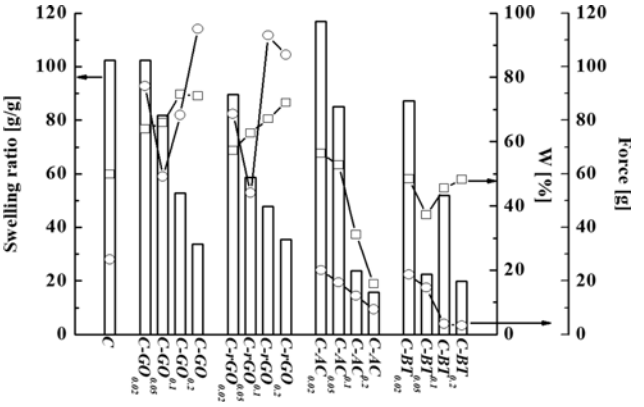

Fig. 5. Gel strength (○), gel fraction (□), and equilibrium swelling ratio (bar) of the prepared materials in distilled water.

respectively, while ***C-AC***$_{0.2}$ and ***C-BT***$_{0.2}$ withstood force of 9.3 g and 3.3 g, respectively. As the amount of AC and BT increased, gel strength decreased. It can be confirmed that the inorganic composite superabsorbents with GO and rGO had higher strength than the composite superabsorbents with AC or BT. In addition, the addition of GO and rGO increased the gel strength of the prepared superabsorbents, while the addition of AC and BT decreased the gel strength.

2-2. Gel Fraction

Gel fraction was measured to determine the intermolecular crosslinking strength of the prepared inorganic composite superabsorbents (Fig. 5). The pure polymer, ***C***, showed a gel fraction of 49.8%. GO and rGO-added composite superabsorbents had higher gel fraction than ***C***, and AC and BT-added composite superabsorbents showed lower gel fraction than ***C***. The GO-added ***C-GO***$_{0.2}$ showed a gel fraction of 74.2%, which was 10.4% points higher than that of ***C-GO***$_{0.02}$ (63.8%). ***C-rGO***$_{0.2}$ showed a gel fraction of 72.1%, which was increased by 14.9% points from the value of ***C-rGO***$_{0.02}$ (57.2%). Gel fraction increased with increasing GO and rGO content. Contrary to this tendency, AC-added ***C-AC***$_{0.02}$ and ***C-AC***$_{0.2}$ showed 56.3% and 15.8% of gel fractions, respectively, and the gel fraction decreased with increasing AC content. ***C-BT***$_{0.02}$ and ***C-BT***$_{0.2}$ showed gel fractions of 48.4% and 48.1%, respectively, and the change in the BT contents did not significantly affect the gel fraction of the prepared composite superabsorbents. As the amount of GO and rGO added increased, the gel fraction of the prepared composite superabsorbents increased. However, AC and BT-added materials showed opposite trends. These results are consistent with the gel strength measurement results described above. This seems to be because a large amount of functional groups present on the surface of GO and rGO combined with CMC polymer to increase the strength of the prepared composite superabsorbents. Although it is the same carbon material, it seems that AC does not

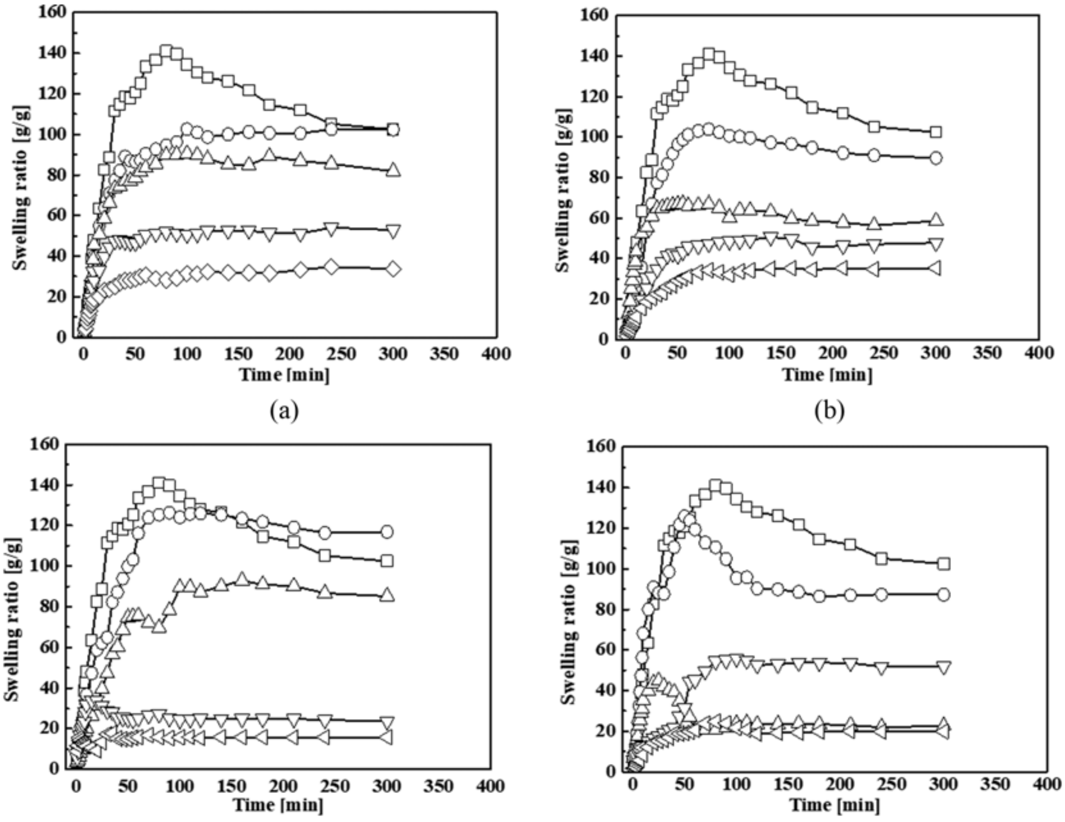

(a) (b)

(c) (d)

Fig. 6. Swelling kinetics of *C* (□), *C-I*$_{0.02}$ (○), *C-I*$_{0.05}$ (△), *C-I*$_{0.1}$ (▽), and *C-I*$_{0.2}$ (◁) in distilled water (inorganic additives, I: GO (a), rGO (b), AC (c), and BT (d)).

form a bond with CMC polymer due to the small amount of surface functional groups, but rather reduces the strength of the prepared composite superabsorbents.

2-3. Swelling Kinetics

Swelling ratio changes with time were measured to determine swelling rate and equilibrium swelling ratio of the prepared inorganic composite superabsorbents. The swelling test results of the prepared superabsorbents in distilled water are shown in Fig. 6. The pure polymer ***C*** reached a maximum swelling ratio of 141.0 g/g at 80 minutes. However, the structure of the swollen gel collapsed and the superabsorbent leached out of the tea bag, and the swelling ratio decreased to about 102.5 g/g after 300 minutes, which was about 27.3% lower than the maximum value. Structure of the BT-added superabsorbents also collapsed after reaching the maximum swelling ratio (Fig. 6(d)). On the contrary, superabsorbents with GO, rGO, and AC reached maximum swelling ratios within 110, 90 and 110 minutes in all compositions, respectively. After then the swelling ratios remained unchanged without decreasing. In addition, it was observed that the maximum swelling ratio of superabsorbents decreased as the amount of inorganic additive increased. The swelling kinetics of the prepared superabsorbents in urea aqueous solution (50 g/L) and NaCl aqueous solution (9 g/L) was also measured. The results of the experiments were similar to those of the tests in distilled water and are shown in Supporting Information (Fig. S5 and Fig. S6). Swelling rate experiments were performed until no change in swelling ratio was observed, and the last measured values were used as the equilibrium swelling ratios in the following.

2-4. Equilibrium Swelling Ratio

The equilibrium swelling ratios of the prepared inorganic composite superabsorbents in distilled water, urea aqueous solution and NaCl aqueous solution are shown in Fig. 7. In most superabsorbents, the equilibrium swelling ratio decreased in the order of distilled water, urea aqueous solution and NaCl aqueous solution. Especially, the equilibrium swelling ratio was the lowest in the NaCl aqueous solution. This is presumably due to the phenomenon that the Na^+ ion of the NaCl aqueous solution exhibits a screening effect between the hydrophilic functional group of the superabsorbent and the water molecule, thereby depriving the water molecule space in the superabsorbent [15,25]. In addition, the equilibrium swelling ratios of the prepared superabsorbents tended to decrease as the amount of the added inorganic material increased. This tendency was apparent when GO and rGO were used as additives.

The equilibrium swelling ratios of the prepared superabsorbents in distilled water are shown in Fig. 5 together with the gel strength and gel fraction. In the composite superabsorbents with GO and rGO, gel strength and gel fraction increased with the increase of the amount of inorganic additives added. However, equilibrium swelling ratios decreased with the opposite trend. However, gel strength, gel fraction and equilibrium swelling ratio of the composite superabsorbents containing AC decreased as the amount of the added AC increased. As the amount of added BT increased in the BT-added superabsorbents, gel strength and equilibrium swelling ratio decreased, and gel fraction showed no significant difference regardless of the amount of the inorganic additive. According to Qiu et al. [10], gel fraction could be increased by increasing the amount of inorganic additives. However, swelling ratio tended to decrease as the amount of inorganic additive increased. In this work, it was expected that increasing the amount of inorganic additives would increase gel strength and gel fraction and decrease the swelling ratio. The results showed that the composite superabsorbents with GO and rGO added exhibited similar results to what was expected. This tendency is considered to be due to the intermolecular bonding between the three-dimensional structure of the CMC polymer and the surface functional groups of GO and rGO. However, the addition of AC and BT resulted in a decrease in gel strength and gel fraction. Contrary to the case of GO and rGO, AC or BT has a small number of surface functional groups for binding, physically occupies the inside of the polymer structure, and does not form a bond with the CMC polymer, resulting in low gel strength and gel fraction [15].

2-5. Urea Elution

To investigate the applicability of the prepared superabsorents in the field, elution tests were performed using urea as a simulated nitrogen fertilizer. A certain amount of urea was loaded on the prepared composite superabsorbent and eluted in an aqueous solution, and the elution concentrations of urea over time were measured and shown in the Supporting Information (Fig. S7). In most superabsorbents, the urea concentration in the solution reached more than 190 ppm within 2 hours, indicating that the urea over 95% was eluted. The measured kinetic data were plotted on a graph using a

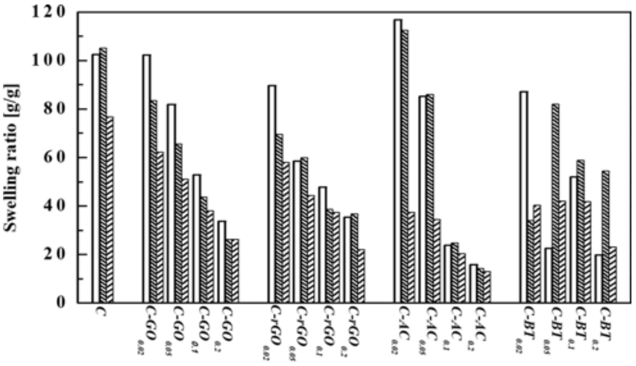

Fig. 7. Equilibrium swelling ratios of the prepared materials in distilled water (☐), 50 g/L urea solution (⧅), and 9 g/L NaCl solution (▨).

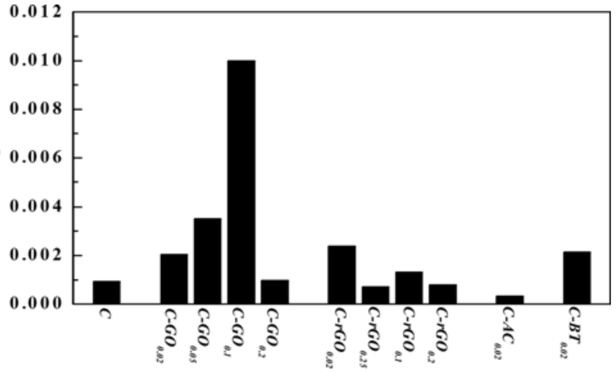

Fig. 8. Urea release rates of the prepared superabsorbents.

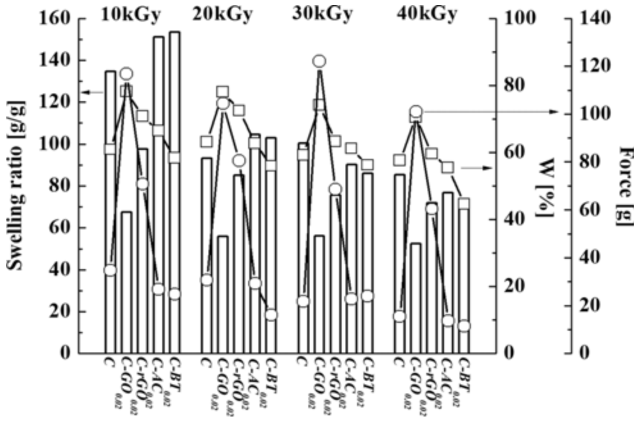

Fig. 9. Gel strength (○), gel fraction (□), and equilibrium swelling ratio (bar) of the materials prepared using different irradiation doses in distilled water.

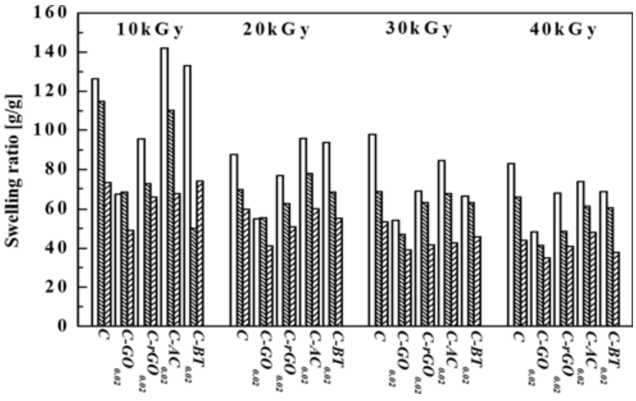

Fig. 10. Equilibrium swelling ratios of the materials prepared using different irradiation doses in distilled water (□), 5 g/L urea solution (▧), and 9 g/L NaCl solution (▨).

pseudo-second-order kinetic model. The rate of urea elution was well fit by the kinetic model, from which the dissolution rate of each superabsorbent was determined and shown in Fig. 8. ***C-GO***$_{0.1}$ showed the fastest dissolution rate, while ***C-AC***$_{0.02}$ showed the slowest dissolution rate. The dissolution rates of most superabsorbents ranged from 0.001 to 0.004 L/mg·min, which was consistent with the literature and suitable for the field application [15].

3. Effect of the Absorbed Dose of Electron Beam Irradiation on Gel Properties

3-1. Gel Strength

Composite superabsorbents were prepared by fixing the amount of inorganic additive to 2% of CMCNa mass and changing the absorbed dose of EB irradiation to 10 kGy, 20 kGy, 30 kGy and 40 kGy, respectively (Table 1). Gel strength of the prepared composite superabsorbent in the swollen state was measured and shown in Fig. 9. The pure polymer ***C*** showed a maximum value of 34.9 g when irradiated at 10 kGy and the lowest value of 15.5 g when irradiated at 40 kGy. ***C-GO***$_{0.02}$ was able to withstand the maximum value of 122.0 g when irradiated at 30 kGy and the lowest value of 100.9 g when irradiated at 40 kGy. ***C-rGO***$_{0.02}$ was able to withstand a maximum force of 80.6 g when irradiated at 20 kGy and a lowest force of 60.4 g when irradiated at 40 kGy. ***C-AC***$_{0.02}$ withstood 29.2 g at 20 kGy, and ***C-BT***$_{0.02}$ withstood 24.7 g and 11.4 g at 10 kGy and 40 kGy, respectively, showing very low gel strength. ***C-GO***$_{0.02}$ showed about 3.5-times and ***C-rGO***$_{0.02}$ showed about 2.7-times higher gel strength than pure polymer ***C***. ***C-GO***$_{0.02}$ showed the highest gel strength at all absorbed doses of EB irradiations, and gel strength decreased in the order of ***C-rGO***$_{0.02}$, ***C***, ***C-AC***$_{0.02}$, and ***C-BT***$_{0.02}$. Generally, superabsorbents prepared at 10 kGy showed the highest gel strength, and gel strength decreased with increasing the absorbed dose of EB irradiation. These results showed similar tendency to the gel fraction test results shown below.

3-2. Gel Fraction

Gel fractions of the prepared composite superabsorbents are shown in Fig. 9. ***C***, a pure polymer, exhibited a gel fraction of 57.6% or more at all absorbed doses of EB irradiations. ***C-GO***$_{0.02}$ showed the highest gel fraction of 78.0% when irradiated at 10 kGy and showed a gel fraction of 70.5% at 40 kGy. Similarly, ***C-rGO***$_{0.02}$ showed high gel fractions of 70.8% and 72.4% at 10 kGy and 20 kGy, respectively, but a low gel fraction of 59.5% at 40 kGy. ***C-AC***$_{0.02}$ showed the highest gel fraction (66.4%) at 10 kGy and the lowest gel fraction (55.5%) at 40 kGy. ***C-BT***$_{0.02}$ also showed a similar tendency (58.3% at 10 kGy and 44.5% at 40 kGy). Generally, superabsorbents prepared at 10 kGy showed the highest gel fraction, and the gel fraction decreased with increasing the absorbed dose of EB irradiation. In addition, ***C-GO***$_{0.02}$ showed the highest gel fraction, and the gel fraction decreased in the order of ***C-rGO***$_{0.02}$, ***C-AC***$_{0.02}$, ***C***, and ***C-BT***$_{0.02}$.

3-3. Equilibrium Swelling Ratio

Swelling experiments were carried out to determine the swelling rate and equilibrium swelling ratio of the prepared superabsorbents by varying the absorbed dose of EB irradiation. Swelling rate experimental results are shown in the Supporting Information (Fig. S8-Fig. S10). Equilibrium swelling ratios of the composite superabsorbents in distilled water, urea aqueous solution and NaCl aqueous solution are shown in Fig. 10. Superabsorbent prepared by irradiation of EB at 10 kGy exhibited the highest equilibrium swelling ratio, and the equilibrium swelling ratio decreased as the absorbed dose increased. GO-added superabsorbents did not have large equilibrium swelling ratios in the aqueous solutions as compared with other superabsorbents. However, they showed the smallest decrease in the equilibrium swelling ratio with the increase of the absorbed dose of EB irradiation among the superabsorbents used in this work. Equilibrium swelling ratio, gel strength and gel fraction of the superabsorbents in distilled water are shown together in Fig. 9. As previously described, superabsorbents prepared by irradiation of EB at 10 kGy showed the highest equilibrium swelling ratio, gel strength and gel fraction values.

3-4. Urea Elution

Urea elution tests were also carried out, and the results are shown in the Supporting Information (Fig. S11-Fig. S15). Most superabsorbents showed urea elution over 180 ppm between 60 and 120 minutes, indicating that more than 90% of the loaded urea was eluted within two hours. Elution rate constants of the superabsorbents obtained using pseudo-second-order kinetic model ranged from 0.0005 to 0.002 L/mg·min (Fig. 11). These values are similar to the conventional elution rates, showing no significant differ-

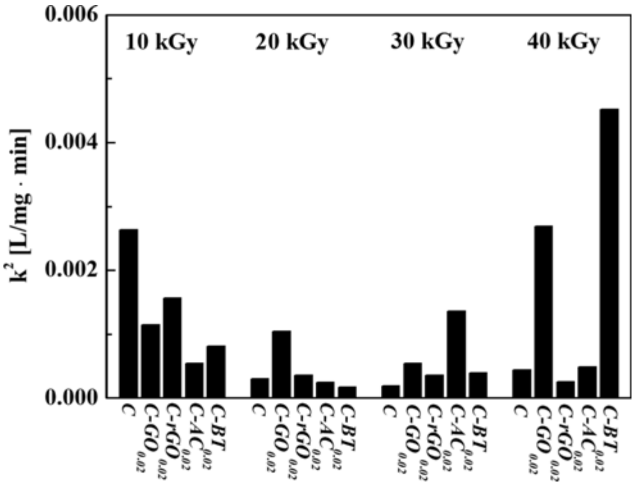

Fig. 11. Urea release rates of the superabsorbents prepared using different irradiation doses.

ences even when the absorbed dose of EB irradiations changed [15].

4. Effect of the Types of Radiation on Gel Properties

4-1. Gel Strength

In this work, EB was used to fabricate composite superabsorbents. To produce a superabsorbent, γ-ray can be also used as a radiation source instead of EB. In general, when γ-rays are used, the irradiation time should be longer than EB. However, the transmittance of γ-rays is high, so that a large amount of superabsorbent can be produced by γ-ray irradiation [6]. However, EB is not suitable for mass production of superabsorbents due to the low transmittance, but it has a short irradiation time. The effect of different types of radiation on the properties of the composite superabsorbent was investigated. As shown in Table 1, the amounts of CMCNa and inorganic materials used were kept constant in the preparation of superabsorbents, and the intensities and absorbed doses of EB and γ-ray irradiations were also kept constant at 0.7 MeV and 10 kGy, respectively. Gel strength of the inorganic composite superabsorbent prepared by using γ-ray and EB is shown in Fig. 12. Among the prepared materials, $\boldsymbol{C\text{-}GO_{0.02}\text{-}e}$ prepared by irradiating EB showed the highest gel strength of 65.1 g. Gel strengths of the superabsorbents were high in the order of $\boldsymbol{C\text{-}GO_{0.02}\text{-}e}$, $\boldsymbol{C\text{-}rGO_{0.02}\text{-}e}$, $\boldsymbol{C\text{-}GO_{0.02}\text{-}\gamma}$, ***C-e***, $\boldsymbol{C\text{-}rGO_{0.02}\text{-}\gamma}$, and $\boldsymbol{C\text{-}\gamma}$. Composite superabsorbents prepared by irradiation of EB showed higher gel strength than the superabsorbents prepared by irradiation of γ-rays. While γ-rays have higher permeability than other radiation, their ionization efficiency is poor [6]. However, EB is less permeable than γ-rays but has a high ionization efficiency. For this reason, it was considered that the composite superabsorbents with higher gel strength were obtained by the EB irradiation rather than γ-ray irradiation.

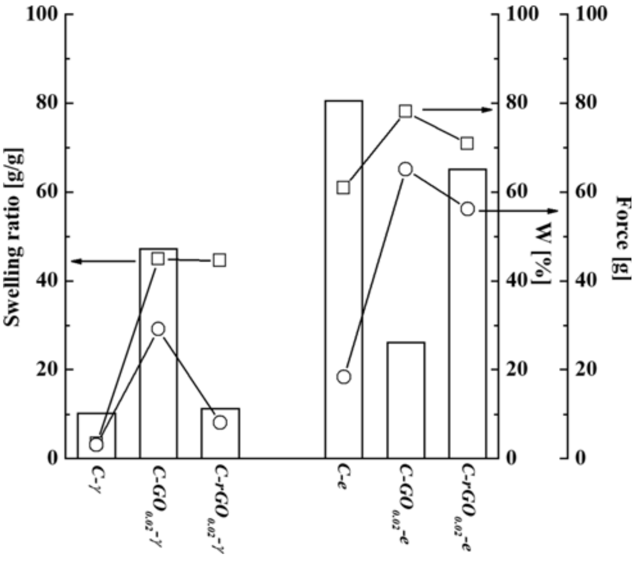

Fig. 12. Gel strength (○), gel fraction (□), and equilibrium swelling ratio (bar) of the materials prepared using γ-ray and electron beam in distilled water.

4-2. Gel Fraction

Gel fractions were also measured on the inorganic composite superabsorbents prepared by irradiating γ-rays and EBs (Fig. 12). $\boldsymbol{C\text{-}\gamma}$, a pure polymer prepared by irradiation of γ-rays, showed a low gel fraction of 3.3%, indicating that it had little function as a superabsorbent. However, ***C-e*** produced by EB showed a relatively high gel fraction of 60.8%. $\boldsymbol{C\text{-}GO_{0.02}\text{-}\gamma}$ exhibited a gel fraction of 44.8% and $\boldsymbol{C\text{-}GO_{0.02}\text{-}e}$ showed a higher gel fraction of 78.0%, respectively. Among the composite superabsorbents with rGO added, the superabsorbent prepared by irradiating EB also showed a higher gel fraction ($\boldsymbol{C\text{-}rGO_{0.02}\text{-}e}$, 70.8%) than that irradiated with γ-ray ($\boldsymbol{C\text{-}rGO_{0.02}\text{-}\gamma}$, 44.5%). According to Wach et al., the gel fraction of superabsorbent prepared by γ-irradiation at low absorbed dose was about 10% higher than that prepared using EB. They also reported that there was no significant difference in the gel fraction between the superabsorbents prepared by γ-rays and by EB [9]. In this work, we used the absorbed dose of 10 kGy, so it was expected that the gel fraction when γ-rays were used would be higher than that of EB. However, the EB-irradiated samples exhibited gel fraction and gel strength several times higher than those irradiated with γ-rays. This is probably because EB produced a larger amount of radicals than γ-ray during the preparation of the superabsorbent increasing the degree of cross-linking [6].

4-3. Equilibrium Swelling Ratio

Swelling tests were also carried out in the aqueous solutions to determine the swelling rate and equilibrium swelling ratio of the composite superabsorbents prepared by irradiation of γ-ray and EB. Swelling ratios in each aqueous solution are shown in Fig. 13, and swelling rate experimental results are shown in the Supporting Information (Fig. S16-Fig. S18). In distilled water, ***C-e*** showed the largest swelling ratio of 80.4 g/g, and the swelling ratio decreased in the order of $\boldsymbol{C\text{-}rGO_{0.02}\text{-}e}$, $\boldsymbol{C\text{-}GO_{0.02}\text{-}\gamma}$, $\boldsymbol{C\text{-}GO_{0.02}\text{-}e}$, $\boldsymbol{C\text{-}rGO_{0.02}\text{-}\gamma}$, and $\boldsymbol{C\text{-}\gamma}$. $\boldsymbol{C\text{-}\gamma}$ and $\boldsymbol{C\text{-}rGO_{0.02}\text{-}\gamma}$ collapsed during the swelling process, resulting in the loss of superabsorbent and very low swelling ratio ($\boldsymbol{C\text{-}\gamma}$, 10.5 g/g). Similar trends were observed in urea aqueous solution and NaCl aqueous solution. Generally, swelling ratios of the superabsorbents irradiated with EB was higher than those of the superabsorbents irradiated with γ-ray.

5. Plant Growth

Plant growth experiments were carried out using livestock manure

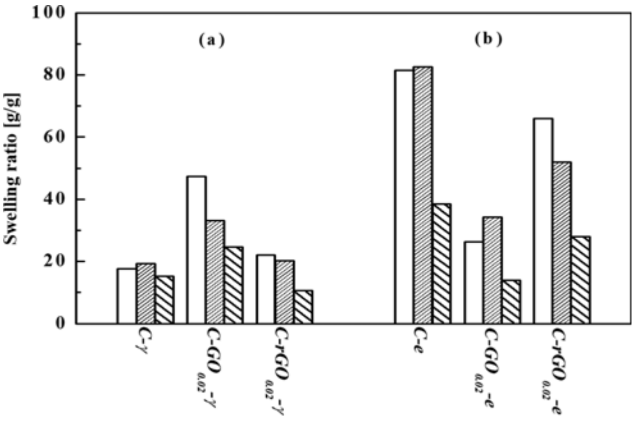

Fig. 13. Equilibrium swelling ratios of the materials prepared using γ-ray (a) and electron beam radiation (b) in distilled water (□), 50 g/L urea solution (▨), and 9 g/L NaCl solution (▧).

to determine the applicability of the prepared superabsorbents. The components of the livestock manure used in the experiment were analyzed according to the standard method. The livestock manure consisted of water (99.01%), potassium (0.21%), salts (0.16%), nitrogen (0.10%), phosphoric acid (0.05%) and small amounts of metals (19.28 ppm zinc, 6.12 ppm copper, 0.30 ppm nickel, 0.16 ppm chromium and 0.04 ppm lead). The pH of the livestock manure was 9.4, COD was 917.5 ppm, and the electrical conductivity was 10.96 mS/cm. Average size of organic particles in the livestock manure was 0.93 μm. Soil was sieved to obtain a size of 1.2 to 4.0 mm for the experiment. The soil was calcined in an oven at 600 °C for three days to remove organic matter (soil A). Soil B was prepared by supporting the livestock manure for ten days on the soil A from which the organic matter was removed. Three types of composite superabsorbents, ***C***, ***C-GO$_{0.02}$***, and ***C-rGO$_{0.02}$***, were used in the experiment. Crown daisy and spinach were used for the cultivation. Crown daisy and spinach were grown on soil A, soil A containing ***C***, soil A containing ***C-GO$_{0.02}$***, and soil A containing ***C-rGO$_{0.02}$***, respectively. The same experiments were also carried out using soil B.

The results of growth of crown daisy are shown in Fig. 14(a). Crown daisy was not sprouted for four weeks in soil A. In soil A containing the composite superabsorbents (***C***, ***C-GO$_{0.02}$***, and ***C-rGO$_{0.02}$***), seeds were sprouted two weeks after planting. They grew by 2.6 to 3.1 cm for four weeks. In soil B, which carried liquid fertilizer, seeds were sprouted after three weeks. In soil B containing the composite superabsorbents (***C***, ***C-GO$_{0.02}$***, and ***C-rGO$_{0.02}$***), shoots sprouted two weeks later and grown 2.2 to 4.6 cm. Spinach sprouted three weeks after starting the experiment in soil A and grew to 4.0 cm at four weeks (Fig. 14(b)). In soil A containing ***C-GO$_{0.02}$***, spinach sprouted three weeks later and grew to 6.6 cm at four weeks. In soil A containing ***C-rGO$_{0.02}$***, shoots were grown three weeks later and grew to 4.2 cm at four weeks. In soil B with livestock manure, shoots grew to 4.0 cm at four weeks. In soil B containing the composite superabsorbents (***C***, ***C-GO$_{0.02}$***, and ***C-rGO$_{0.02}$***), shoots were grown two weeks later and grew by 4.2 to 5.5 cm at four weeks.

When both plants were grown in the soil mixed with the composite superabsorbents, the buds were formed about one week earlier and the stem was slightly larger than those in the soil with no composite superabsorbents. It is considered that this is because the composite superabsorbent in the soil was swollen and the absorbed moisture was gradually released to help the growth of the plant. In addition, plant growth was faster when soil B, which contained livestock manure, was used with composite superabsorbents. This suggests that the composite superabsorbent absorbed water and livestock manure and released them slowly, which helped the plant growth.

CONCLUSIONS

Composite superabsorbents were successfully prepared using EB irradiation as the slow-release liquid fertilizer. To investigate the effect of inorganic additives on the physical properties of the superabsorbents, four kinds of additive materials were used, including GO, rGO, AC, and BT. Among them, superabsorbents with GO and rGO showed high gel fraction and high mechanical strength.

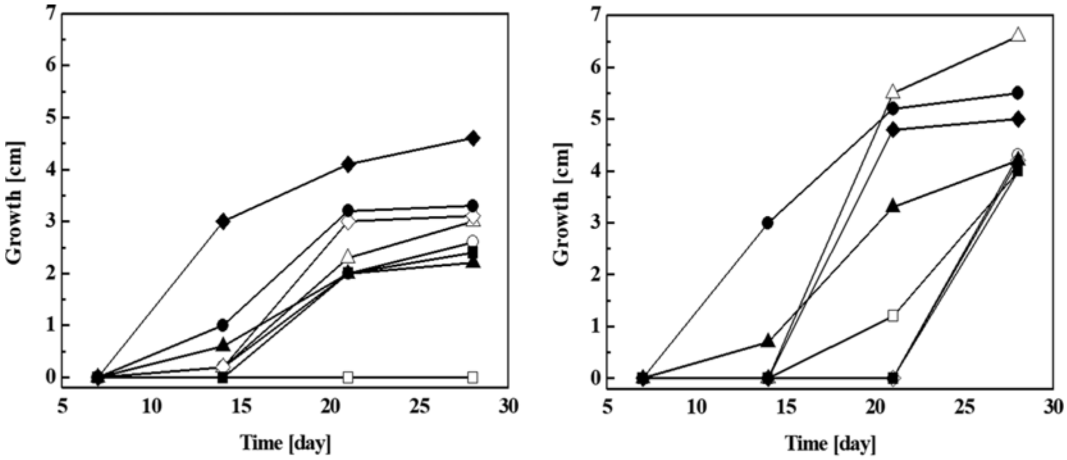

(a) (b)

Fig. 14. Growing of (a) crown daisy and (b) spinach in soil A (□), soil A containing *C* (○), soil A containing *C-GO$_{0.02}$* (△), soil A containing *C-rGO$_{0.02}$* (◇), soil B (■), soil B containing *C* (●), soil B containing *C-GO$_{0.02}$* (▲), and soil B containing *C-rGO$_{0.02}$* (◆).

Gel strength and gel fraction increased with the increase of the amount of GO and rGO added but the equilibrium swelling ratio decreased. These results are considered to be due to the intermolecular bonding between the three-dimensional structure of the CMC polymer and the surface functional groups of GO and rGO. However, the addition of AC and BT resulted in a decrease in gel strength and gel fraction. AC or BT has a small number of surface functional groups for binding and does not form a bond with the CMC polymer. In addition, the effect of the absorbed dose of EB irradiation on gel properties was investigated. Superabsorbents prepared at 10 kGy showed the highest gel strength and gel fraction, but these values decreased with increasing EB irradiation. Superabsorbents prepared by irradiation of EB at 10 kGy also exhibited the highest equilibrium swelling ratio, but the equilibrium swelling ratio decreased as the absorbed dose increased. Furthermore, the effect of the type of radiation on gel properties was also investigated. Composite superabsorbents prepared by EB irradiation showed higher gel strength than those prepared by γ-ray irradiation. From the experimental results, it was possible to derive the optimal conditions for manufacturing the composite superabsorbent. GO or rGO, which was rich in surface functionality, was used in an amount of 0.02 based on the mass of CMC, considering both the mechanical strength and swelling ratio of the superabsorbent. By irradiating an EB of 10 kGy, which was the smallest dose absorbed, to the material with this composition an optimal composite superabsorbent could be prepared. Plant growth was better in the experimental group containing the superabsorbent and the liquid fertilizer. This shows that carbon composite superabsorbent can function as a slow-release liquid fertilizer without falling down of gel structure in soil to help plant growth by absorbing and releasing moisture and liquid fertilizer.

ACKNOWLEDGEMENT

This research was supported by the Bisa Research Grant of Keimyung University in 2019.

SUPPORTING INFORMATION

Additional information as noted in the text. This information is available via the Internet at http://www.springer.com/chemistry/journal/11814.

REFERENCES

1. 1996 Protocol to the Convention on the Prevention of Marine Pollution by Dumping of Wastes and Other Matter (as amended in 2006).
2. National Institute of Animal Science Korea, Liquefaction of livestock manure. http://www.nias.go.kr/envi/DataFileDown.do?fileid=14004, 2008 (accessed 1 November 2016).
3. M. J. Zohuriaan-Mehr and K. Kabiri, *Iran. Polym. J.*, **17**, 451 (2008).
4. C. Chang, B. Duan, J. Cai and L. Zhang, *Eur. Polym. J.*, **46**, 92 (2010).
5. S. Francis, D. Mitra, B. R. Dhanawade, L. Varshney and S. Sabharwal, *Radiat. Phys. Chem.*, **78**, 951 (2009).
6. R. L. Clough, *Nucl. Instrum. Methods Phys. Res. Sect. B-Beam Interact. Mater. Atoms*, **185**, 8 (2001).
7. K. Kabiri, H. Omidian, M. J. Zohuriaan-Mehr and S. Doroudiani, *Polym. Compos.*, **32**, 277 (2011).
8. B. Fei, R. A. Wach, H. Mitomo, F. Yoshii and T. Kume, *J. Appl. Polym. Sci.*, **78**, 278 (2000).
9. R. A. Wach, H. Mitomo, F. Yoshii and T. Kume, *J. Appl. Polym. Sci.*, **81**, 3030 (2001).
10. J. Qiu, L. Xu, J. Peng, M. Zhai, L. Zhao, J. Li and G. Wei, *Carbohydr. Polym.*, **70**, 236 (2007).
11. J. Kwon and B. Lee, *Chem. Eng. Res. Des.*, **104**, 519 (2015).
12. Y. Tang, H. Tang, F. Wang, C. Guan and L. Zhu, *Polym. Sci. Ser. B*, **61**, 471 (2019).
13. L. Zhu, Y. Liu, B. Zhou, H. Tang, F. Wang and C. Guan, *Polym. Sci. Ser. B*, **61**, 680 (2019).
14. L. Zhu, Y. Liu, F. Wang, T. He, Y. Tang and J. Yang, *Adv. Polym. Technol.*, **37**, 2885 (2018).
15. Y. Sung, T.-H. Kim and B. Lee, *Macromol. Res.*, **24**, 143 (2016).
16. Y. Sung, T.-H. Kim and B. Lee, *Clean Technol.*, **22**, 258 (2016).
17. D. R. Dreyer, S. Park, C. W. Bielawski and R. S. Ruoff, *Chem. Soc. Rev.*, **39**, 228 (2010).
18. D. C. Marcano, D. V. Kosynkin, J. M. Berlin, A. Sinitskii, Z. Sun, A. Slesarev, L. B. Alemany, W. Lu and J. M. Tour, *ACS Nano*, **4**, 4806 (2010).
19. Y. Huang, M. Zeng, J. Ren, J. Wang, L. Fan and Q. Xu, *Colloid Surf. A-Physicochem. Eng. Asp.*, **401**, 97 (2012).
20. I. Katime, A. Álvarez-Bautista, L. G. Guerrero-Ramírez and E. Mendizábal, *Topol. Supramol. Polym. Sci.*, **1**, 17 (2014).
21. J.-T. Han, S.-Y. Jeong, H.-J. Jeong and G.-W. Lee, *Polym. Sci. Technol.*, **22**, 137 (2011).
22. J.-S. Lee, B.-A. Kim and C.-K. Moon, *J. Korean Soc. Power Syst. Eng.*, **18**, 7 (2014).
23. Y. Seki, A. Altinisik, B. Demircioğlu and C. Tetik, *Cellulose*, **21**, 1689 (2014).
24. S. G. A. Alla, M. Sen and A. W. M. El-Naggar, *Carbohydr. Polym.*, **89**, 478 (2012).
25. K. M. El Salmawi and S. M. Ibrahim, *Macromol. Res.*, **19**, 1029 (2011).

Supporting Information

Optimal synthesis of carboxymethylcellulose-based composite superabsorbents

Byungsu Kim*, **Tak-Hyun Kim****, **and Byunghwan Lee***,†

*Department of Chemical Engineering, Keimyung University, 1095 Dalgubeoldaero, Dalseo-gu, Daegu 42601, Korea
**Advanced Radiation Technology Institute, Korea Atomic Energy Research Institute,
29 Geumgu-gil, Jeongup-si, Jeonbuk 56212, Korea

(*Received 30 July 2020 • Revised 16 September 2020 • Accepted 18 September 2020*)

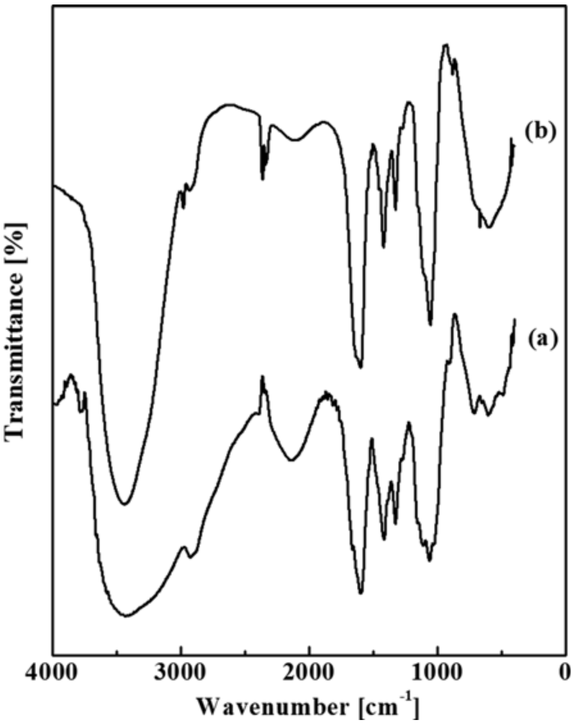

Fig. S1. FTIR spectra of (a) CMCNa and (b) *C*.

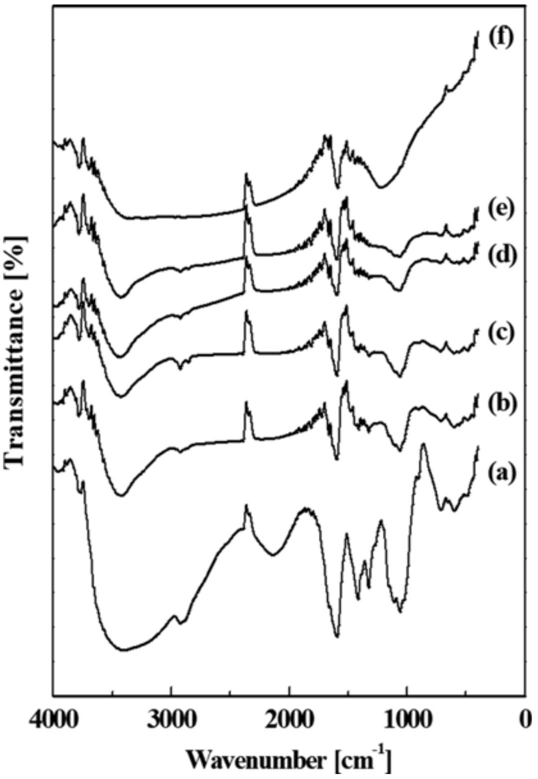

Fig. S2. FTIR spectra of (a) CMCNa, (b) *C-rGO*$_{0.02}$, (c) *C-rGO*$_{0.05}$, (d) *C-rGO*$_{0.1}$, (e) *C-rGO*$_{0.2}$, and (f) rGO.

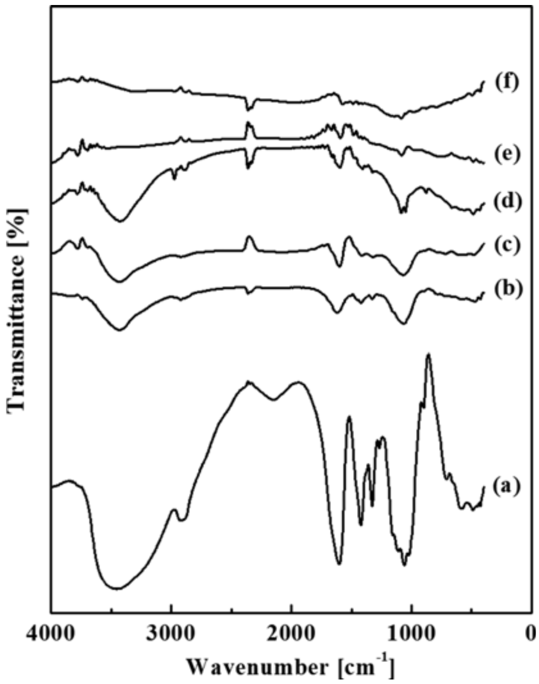

Fig. S3. FTIR spectra of (a) CMCNa, (b) $C\text{-}AC_{0.02}$, (c) $C\text{-}AC_{0.05}$, (d) $C\text{-}AC_{0.1}$, (e) $C\text{-}AC_{0.2}$, and (f) AC.

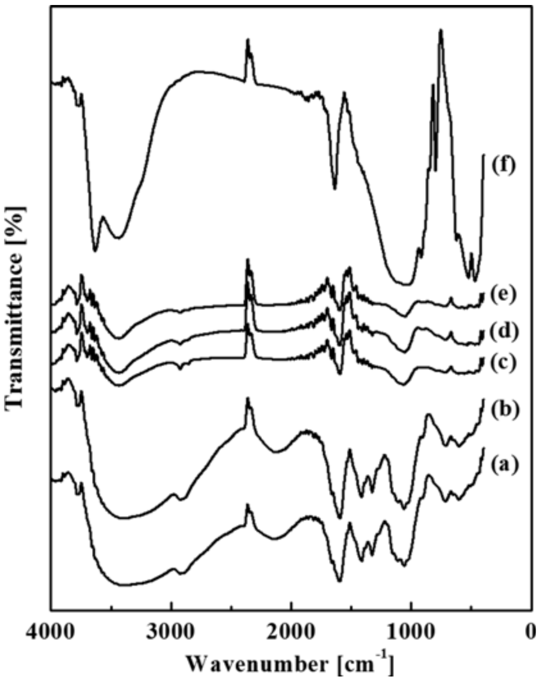

Fig. S4. FTIR spectra (a) CMCNa, (b) $C\text{-}BT_{0.02}$, (c) $C\text{-}BT_{0.05}$, (d) $C\text{-}BT_{0.1}$, (e) $C\text{-}BT_{0.2}$, and (f) BT.

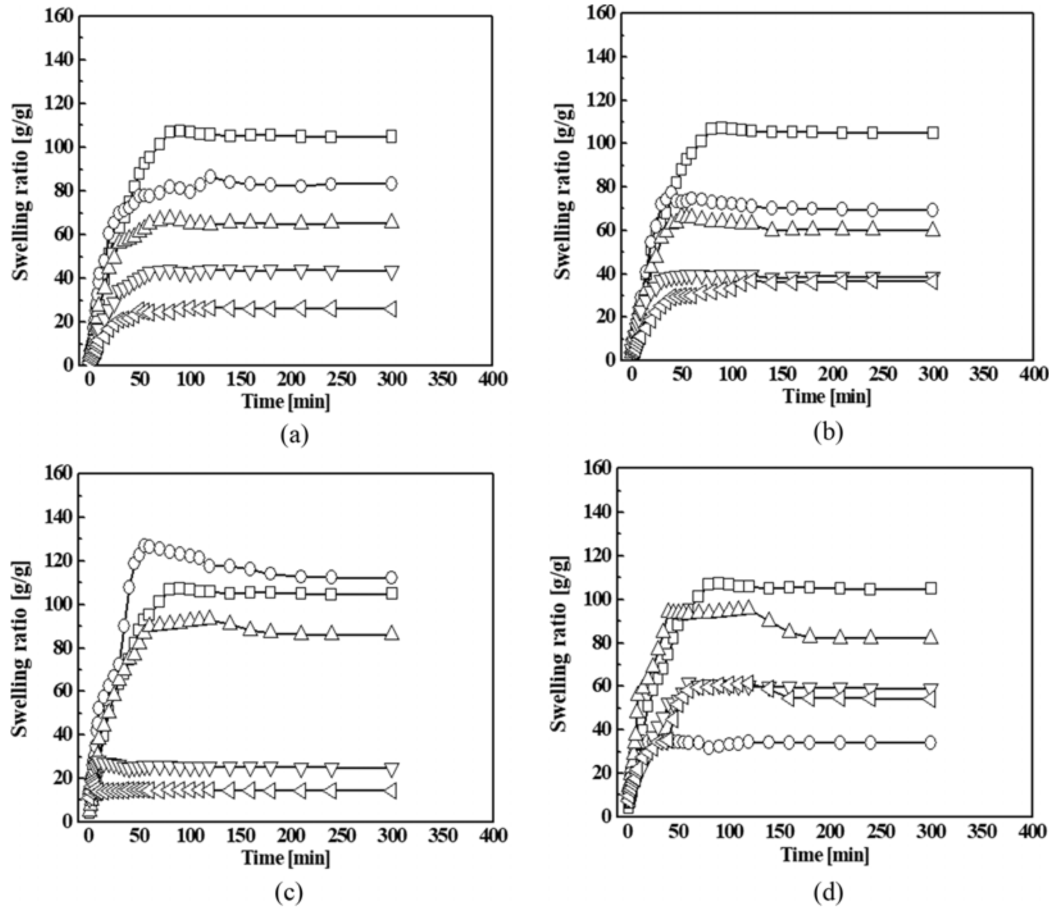

Fig. S5. Swelling kinetics of C (□), $C\text{-}I_{0.02}$ (○), $C\text{-}I_{0.05}$ (△), $C\text{-}I_{0.1}$ (▽), and $C\text{-}I_{0.2}$ (◁) in 50 g/L urea solution (inorganic additives, I: GO (a), rGO (b), AC (c), and BT (d)).

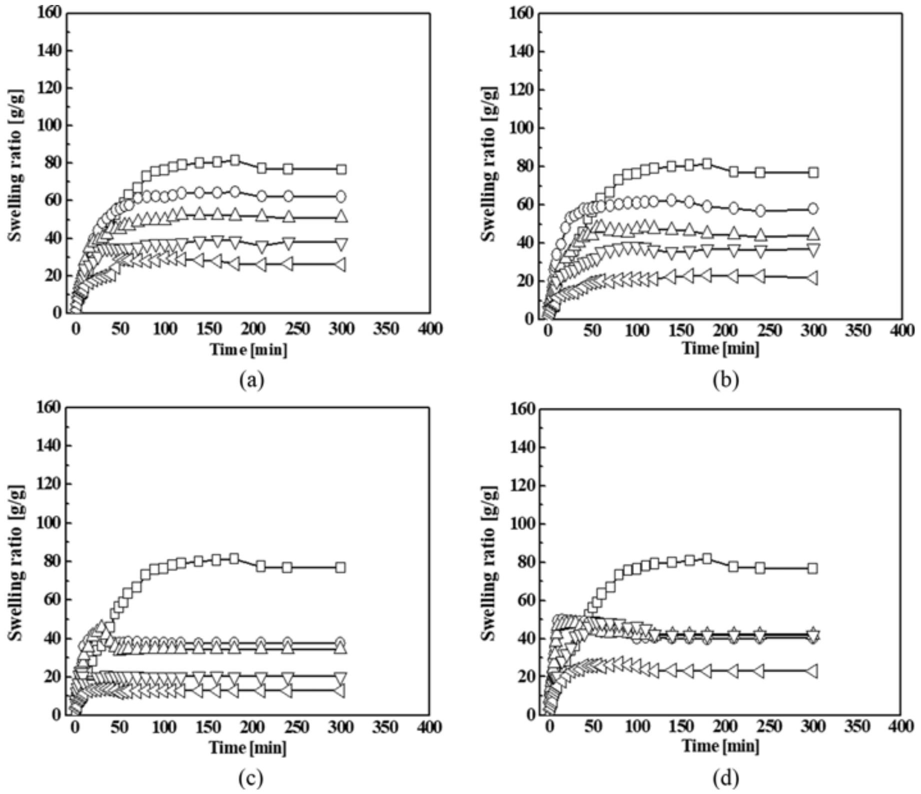

(a) (b) (c) (d)

Fig. S6. Swelling kinetics of C (□), $C\text{-}I_{0.02}$ (○), $C\text{-}I_{0.05}$ (△), $C\text{-}I_{0.1}$ (▽), and $C\text{-}I_{0.2}$ (◁) in 9 g/L NaCl solution (inorganic additives, I: GO (a), rGO (b), AC (c), and BT (d)).

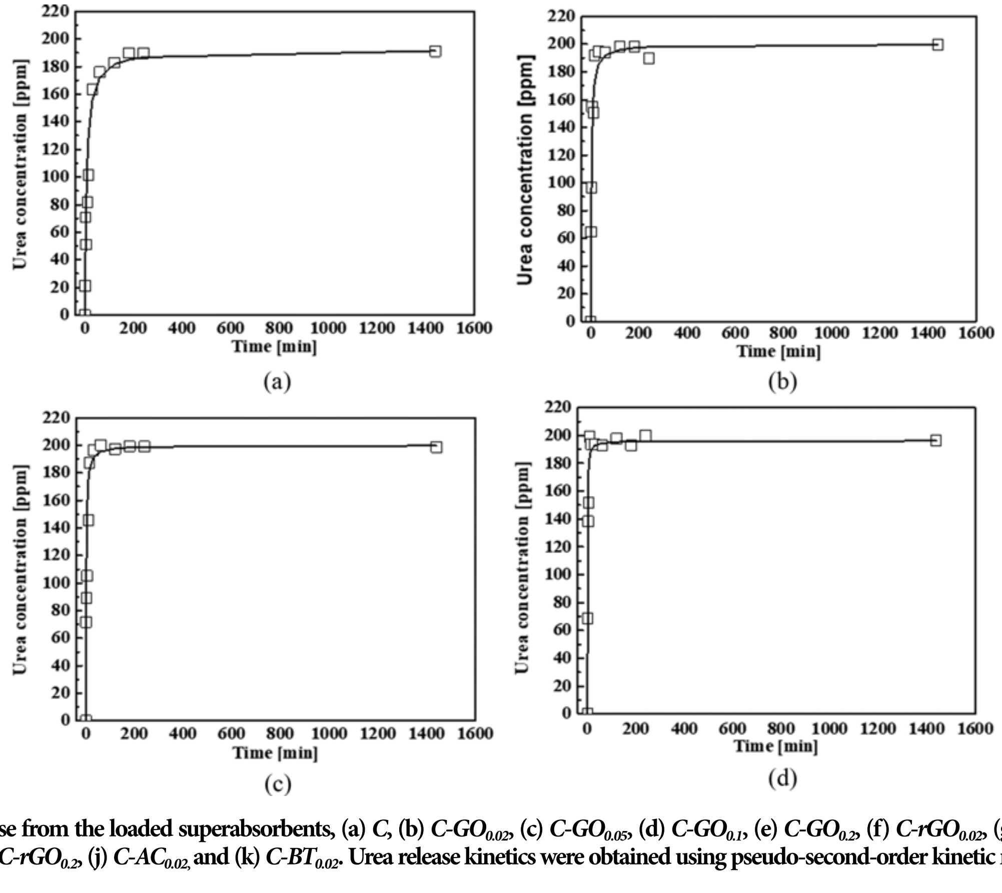

(a) (b) (c) (d)

Fig. S7. Urea release from the loaded superabsorbents, (a) C, (b) $C\text{-}GO_{0.02}$, (c) $C\text{-}GO_{0.05}$, (d) $C\text{-}GO_{0.1}$, (e) $C\text{-}GO_{0.2}$, (f) $C\text{-}rGO_{0.02}$, (g) $C\text{-}rGO_{0.05}$, (h) $C\text{-}rGO_{0.1}$, (i) $C\text{-}rGO_{0.2}$, (j) $C\text{-}AC_{0.02}$, and (k) $C\text{-}BT_{0.02}$. Urea release kinetics were obtained using pseudo-second-order kinetic model (solid lines).

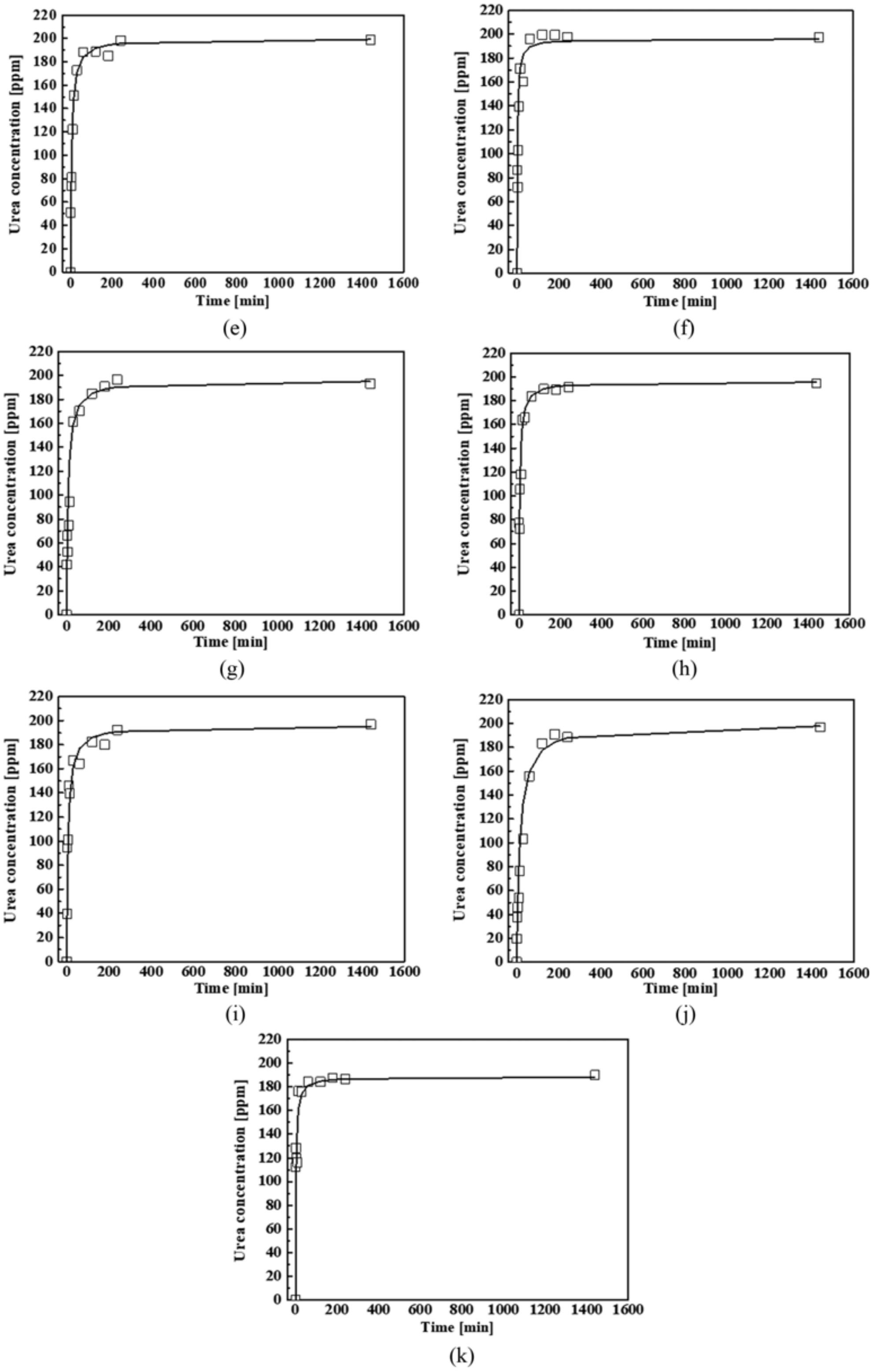

(e) (f) (g) (h) (i) (j) (k)

Fig. S7. Continued.

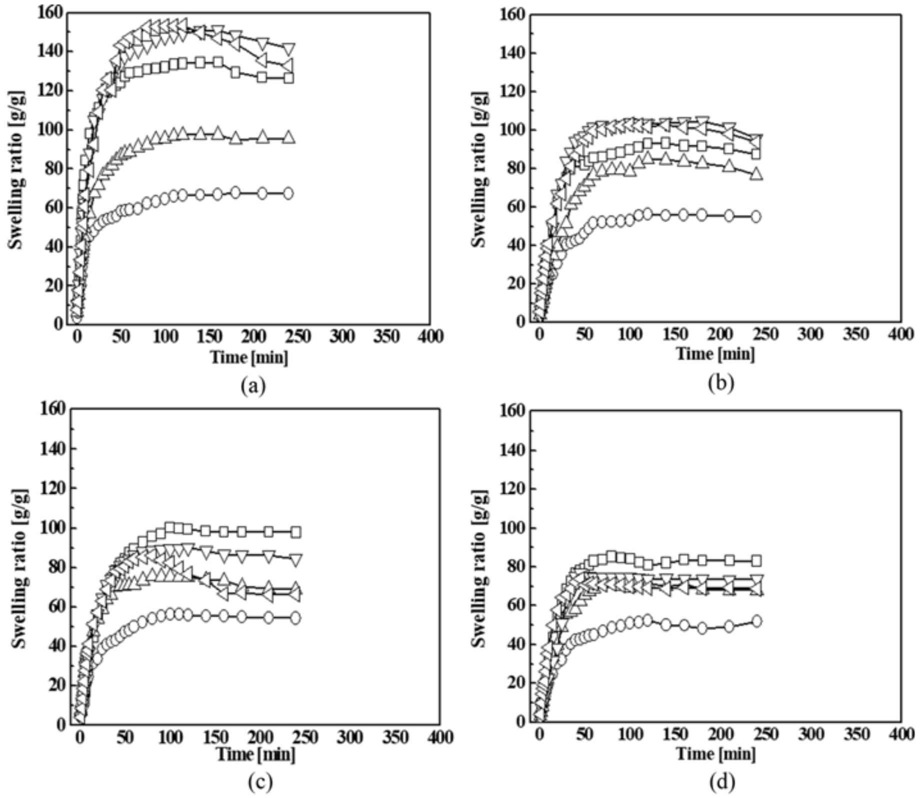

(a)

(b)

(c)

(d)

Fig. S8. Swelling kinetics of the materials prepared using different irradiation doses of (a) 10 kGy, (b) 20 kGy, (c) 30 kGy, and (d) 40 kGy in distilled water: *C* (□), *C-GO$_{0.02}$* (○), *C-rGO$_{0.02}$* (△), *C-AC$_{0.02}$* (▽), and *C-BT$_{0.02}$* (◁).

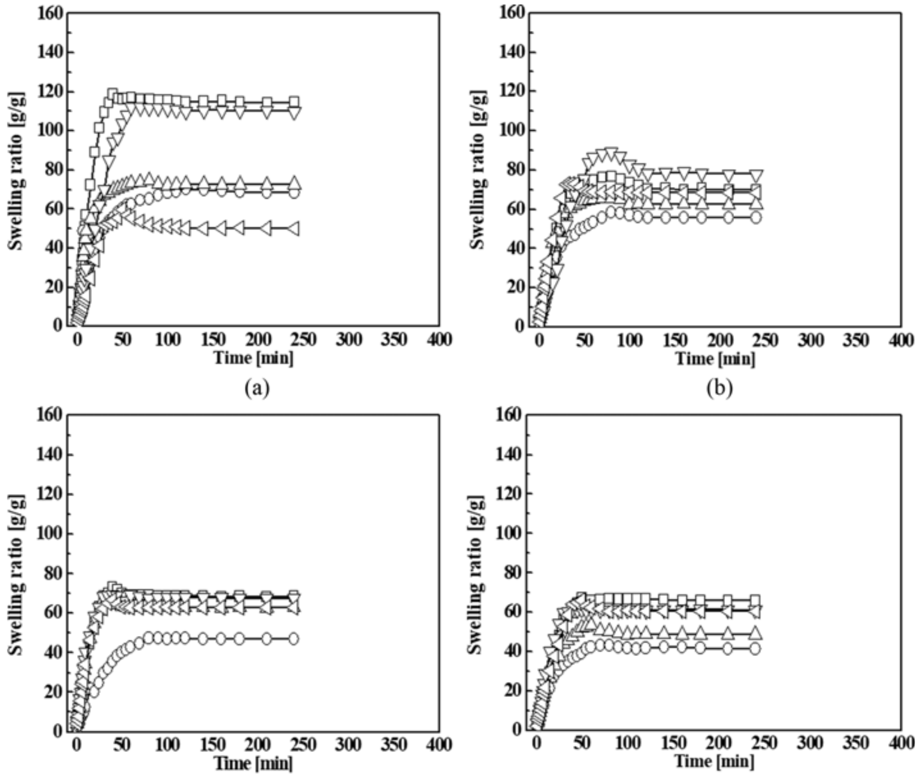

(a)

(b)

(c)

(d)

Fig. S9. Swelling kinetics of the materials prepared using different irradiation doses of (a) 10 kGy, (b) 20 kGy, (c) 30 kGy, and (d) 40 kGy in 50 g/L urea solution: *C* (□), *C-GO$_{0.02}$* (○), *C-rGO$_{0.02}$* (△), *C-AC$_{0.02}$* (▽), and *C-BT$_{0.02}$* (◁).

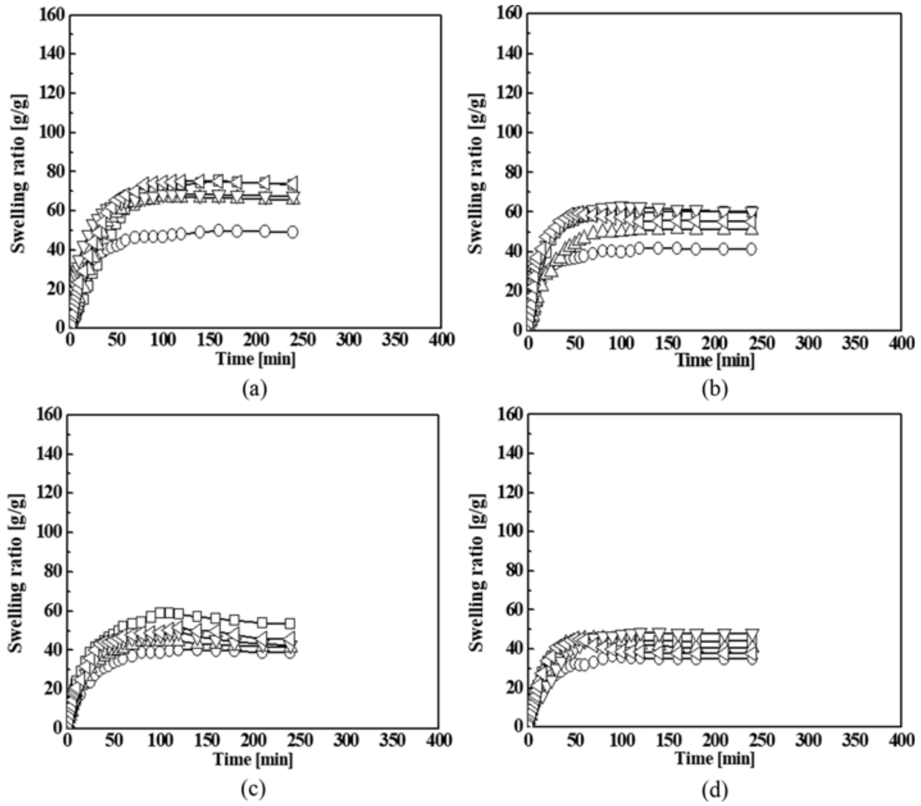

Fig. S10. Swelling kinetics of the materials prepared using different irradiation doses of (a) 10 kGy, (b) 20 kGy, (c) 30 kGy, and (d) 40 kGy in 9 g/L NaCl solution: *C* (□), *C-GO*$_{0.02}$ (○), *C-rGO*$_{0.02}$ (△), *C-AC*$_{0.02}$ (▽), and *C-BT*$_{0.02}$ (◁).

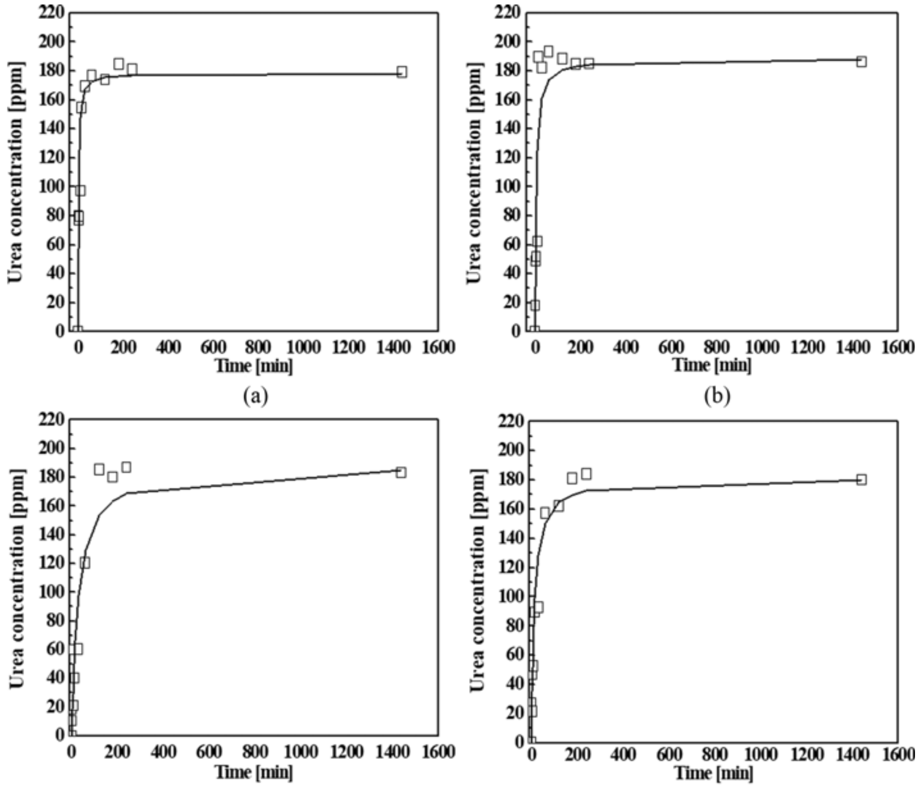

Fig. S11. Urea release from *C* prepared using EB-radiation dose of (a) 10 kGy, (b) 20 kGy, (c) 30 kGy, and (d) 40 kGy.

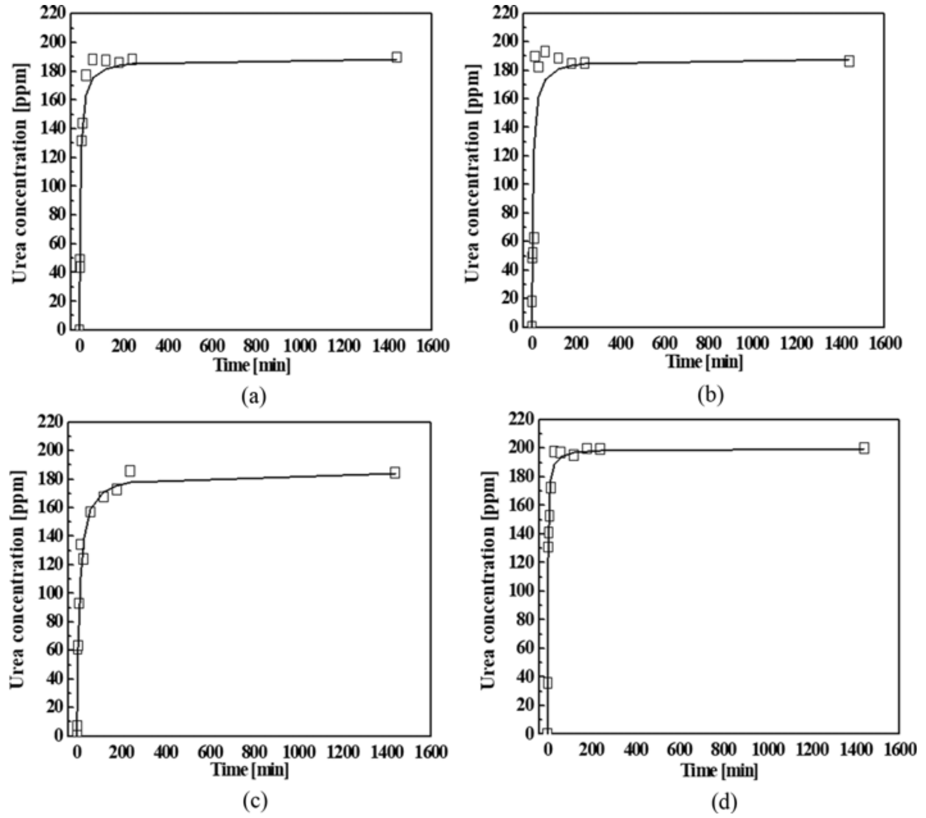

Fig. S12. Urea release from $\mathit{C\text{-}GO}_{0.02}$ prepared using EB-radiation dose of (a) 10 kGy, (b) 20 kGy, (c) 30 kGy, and (d) 40 kGy.

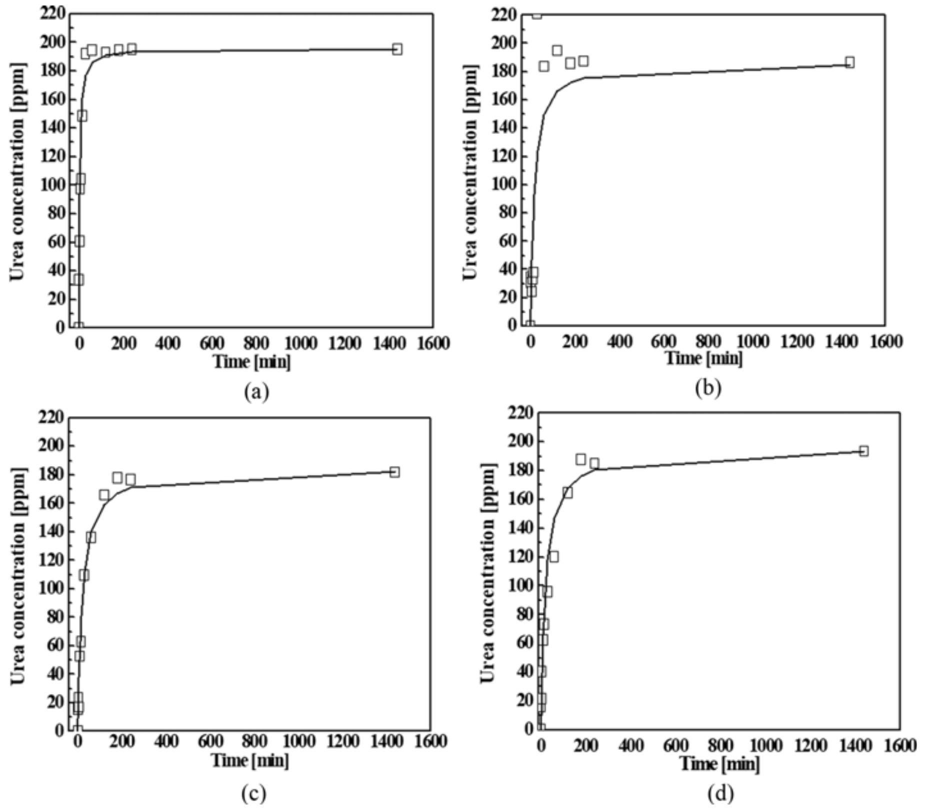

Fig. S13. Urea release from $\mathit{C\text{-}rGO}_{0.02}$ prepared using EB-radiation dose of (a) 10 kGy, (b) 20 kGy, (c) 30 kGy, and (d) 40 kGy.

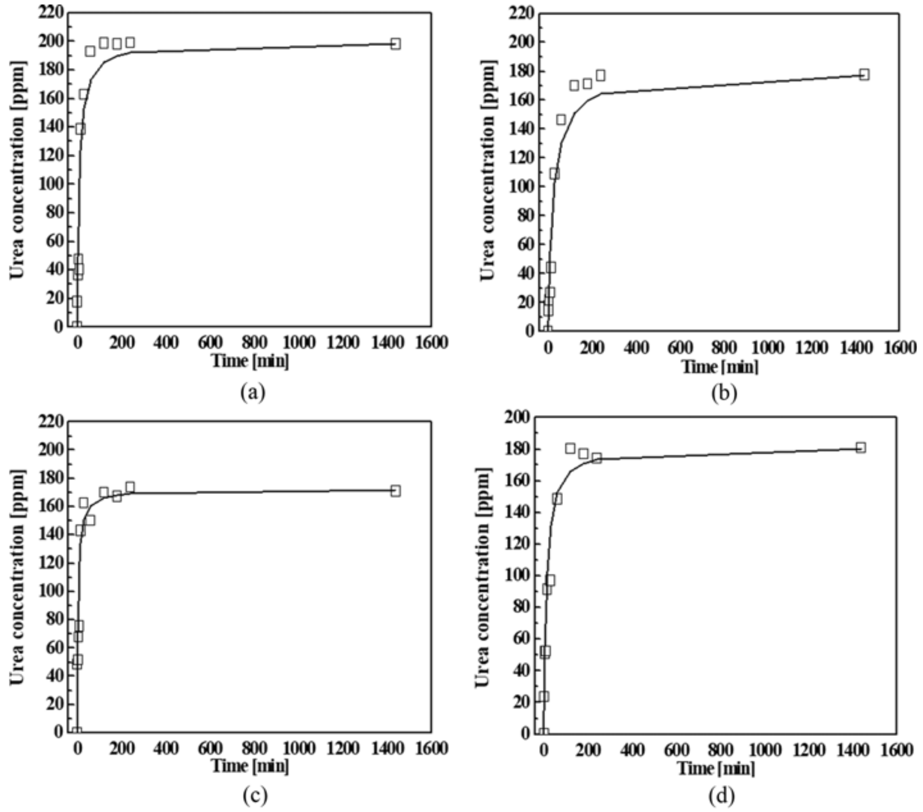

(a) (b) (c) (d)

Fig. S14. Urea release from *C-AC*$_{0.02}$ prepared using EB-radiation dose of (a) 10 kGy, (b) 20 kGy, (c) 30 kGy, and (d) 40 kGy.

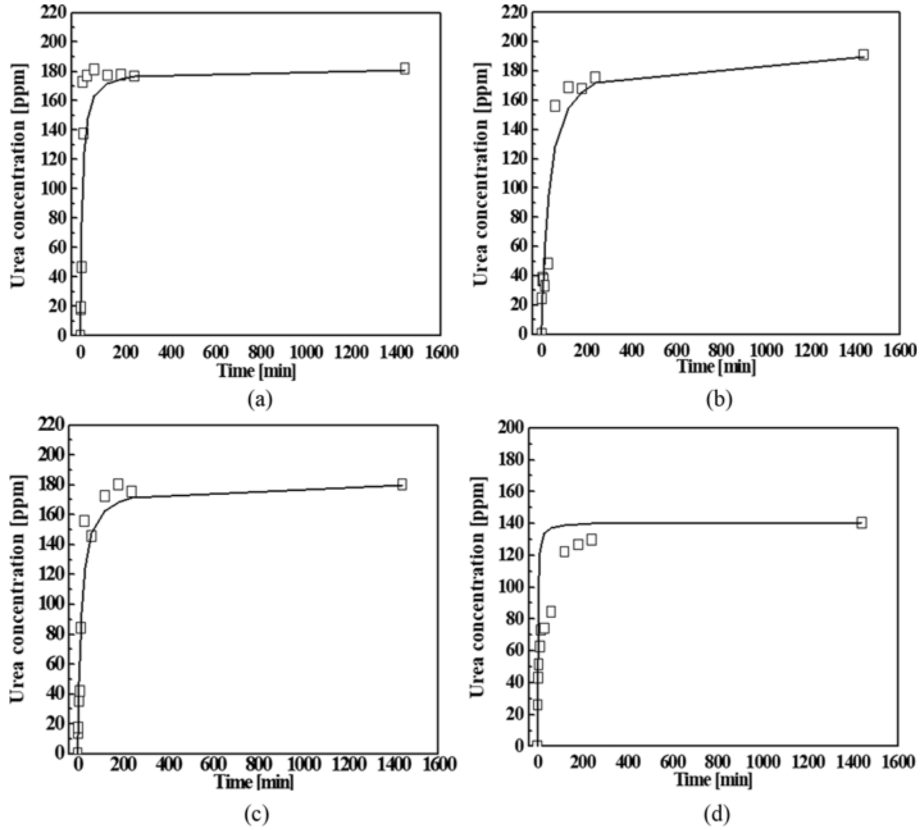

(a) (b) (c) (d)

Fig. S15. Urea release from *C-BT*$_{0.02}$ prepared using EB-radiation dose of (a) 10 kGy, (b) 20 kGy, (c) 30 kGy, and (d) 40 kGy.

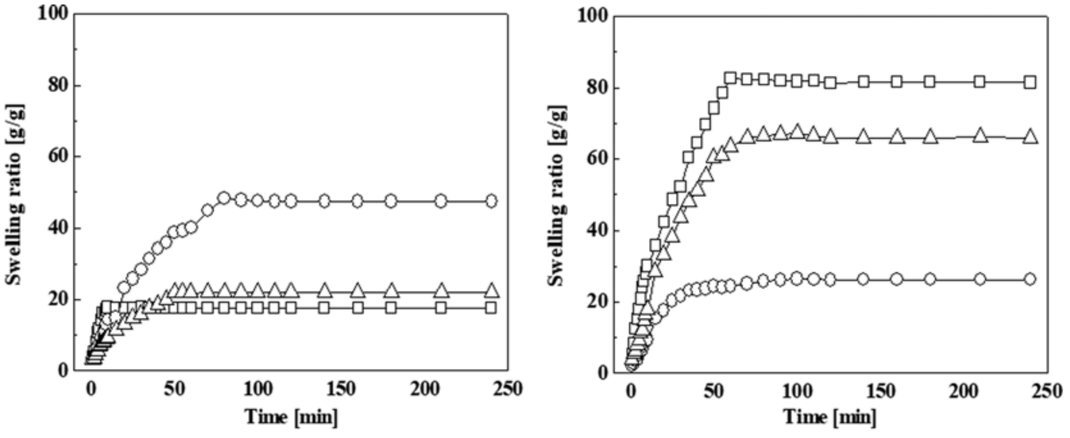

(a) (b)

Fig. S16. Swelling kinetics in distilled water of the materials prepared using γ-ray (a) and electron beam radiation (b): *C* (□), *C-GO*$_{0.02}$ (○), and *C-rGO*$_{0.02}$ (△).

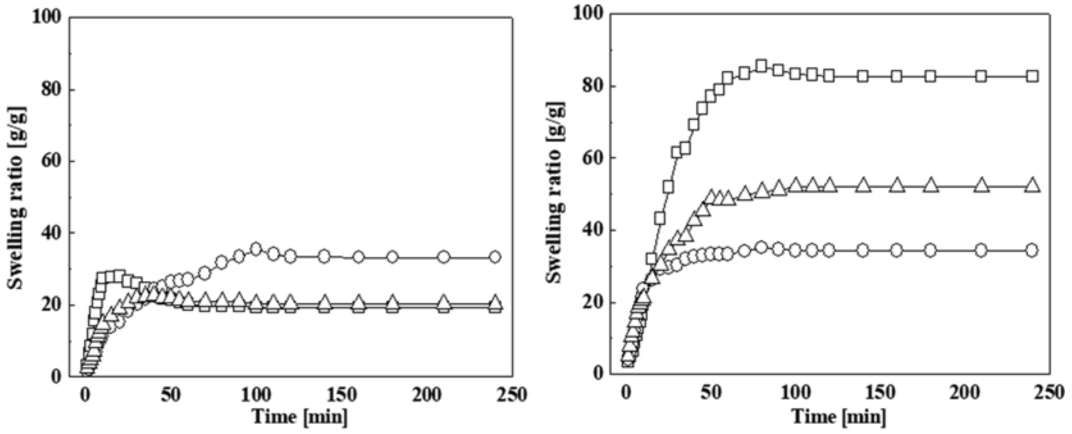

(a) (b)

Fig. S17. Swelling kinetics in 50 g/L urea solution of the materials prepared using γ-ray (a) and electron beam radiation (b): *C* (□), *C-GO*$_{0.02}$ (○), and *C-rGO*$_{0.02}$ (△).

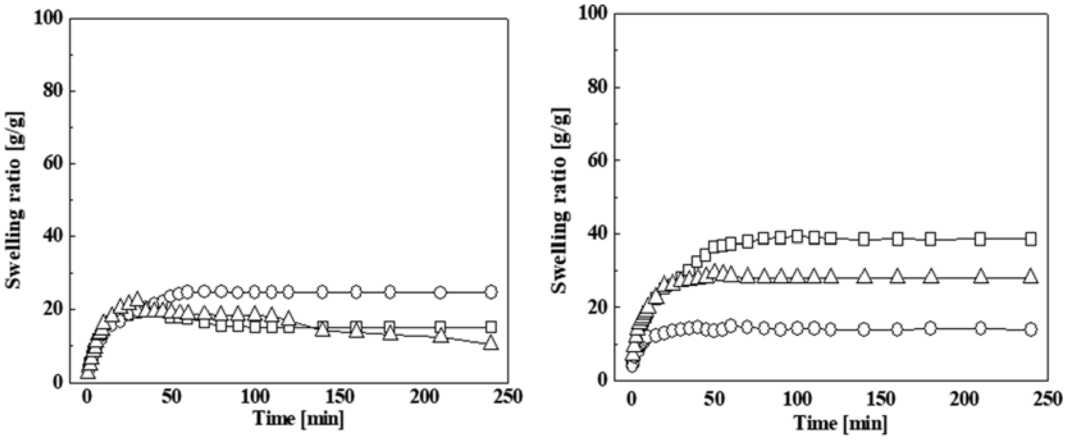

(a) (b)

Fig. S18. Swelling kinetics in 9 g/L NaCl solution of the materials prepared using γ-ray (a) and electron beam radiation (b): *C* (□), *C-GO*$_{0.02}$ (○), and *C-rGO*$_{0.02}$ (△).